USGS
science for a changing world

ECCOE Landsat Quarterly Calibration and Validation Report—Quarter 1, 2022

Open-File Report 2022–1072

U.S. Department of the Interior
U.S. Geological Survey

ECCOE Landsat Quarterly Calibration and Validation Report—Quarter 1, 2022

By Md Obaidul Haque, Rajagopalan Rengarajan, Mark Lubke, Md Nahid Hasan, Fatima Tuz Zafrin Tuli, Jerad L. Shaw, Alex Denevan, Shannon Franks, Esad Micijevic, Michael J. Choate, Cody Anderson, Brian Markham, Kurt Thome, Ed Kaita, Julia Barsi, Raviv Levy, and Lawrence Ong

Open-File Report 2022–1072

U.S. Department of the Interior
U.S. Geological Survey

U.S. Geological Survey, Reston, Virginia: 2022

Suggested citation:
Haque, M.O., Rengarajan, R., Lubke, M., Hasan, M.N., Tuli, F.T.Z., Shaw, J.L., Denevan, A., Franks, S., Micijevic, E., Choate, M.J., Anderson, C., Markham, B., Thome, K., Kaita, E., Barsi, J., Levy, R., and Ong, L., 2022, ECCOE Landsat Quarterly Calibration and Validation report—Quarter 1, 2022: U.S. Geological Survey Open-File Report 2022–1072, 39 p., https://doi.org/10.3133/ofr20221072.

Associated data for this publication:
U.S. Geological Survey, 2021, EarthExplorer: U.S. Geological Survey database, https://earthexplorer.usgs.gov.

ISSN 2331-1258 (online)

Contents

Figures

Tables

Conversion Factors

International System of Units to U.S. customary units

Multiply	By	To obtain
	Length	
nanometer (nm)	0.00000003937	inch (in.)
meter (m)	3.281	foot (ft)
kilometer (km)	0.6214	mile (mi)
kilometer (km)	0.5400	mile, nautical (nmi)
meter (m)	1.094	yard (yd)

Temperature in Kelvin (K) may be converted to degrees Celsius (°C) as follows:

$$°C = K - 273.15.$$

Supplemental Information

Radiance is given in watts per square meter per steradian per micrometer (W/m^2 sr µm).

Within this report, quarter 1 is from January to March, quarter 2 is from April to June, quarter 3 is from July to September, and quarter 4 is from October to December. For example, quarter 1, 2021, was from January to March 2021.

Abbreviations

Please see https://www.usgs.gov/core-science-systems/nli/landsat/glossary-and-acronyms for lists of Landsat glossary terms and other Landsat abbreviations.

~	approximately
ASTER	Advanced Spaceborne Thermal Emission and Reflection Radiometer
CA	coastal/aerosol
Cal/Val	Calibration and Validation
CE90	circular error with 90-percent confidence
CNES	Centre National D'Etudes Spatiales
CPF	calibration parameter file
DOQ	digital orthophoto quadrangle
ECCOE	EROS Cal/Val Center of Excellence
EO	Earth Observation
EROS	Earth Resources Observation and Science
ETM+	Enhanced Thematic Mapper Plus
GCP	ground control point
GRI	Global Reference Image
L0Ra	Level 0 Reformatted Archive
L0Rp	Level 0 Reformatted Product
L1	Level 1
L1C	Sentinel-2 Level-1C
L1T	L1 terrain corrected product
L1TP	L1 Terrain Precision Correction
$L_{typical}$	typical radiance
NEΔT	noise equivalent change in temperature
NIR	near infrared
OLI	Operational Land Imager
PICS	pseudo-invariant calibration sites
RMS	root mean square
RMSE	root mean square error
ROI	region of interest
SNR	signal-to-noise ratio
SPOT	Satellite Pour l'Observation de la Terre
SSM	scene select mechanism
SWIR	shortwave infrared
TIRS	Thermal Infrared Sensor
USGS	U.S. Geological Survey
WRS–2	Worldwide Reference System–2

ECCOE Landsat Quarterly Calibration and Validation Report—Quarter 1, 2022

By Md Obaidul Haque,[1] Rajagopalan Rengarajan,[1] Mark Lubke,[1] Md Nahid Hasan,[1] Fatima Tuz Zafrin Tuli,[1] Jerad L. Shaw,[1] Alex Denevan,[1] Shannon Franks,[1] Esad Micijevic,[2] Michael J. Choate,[2] Cody Anderson,[2] Brian Markham,[3] Kurt Thome,[3] Ed Kaita,[4] Julia Barsi,[4] Raviv Levy,[4] and Lawrence Ong[4]

Executive Summary

The U.S. Geological Survey (USGS) Earth Resources Observation and Science (EROS) Calibration and Validation (Cal/Val) Center of Excellence (ECCOE) focuses on improving the accuracy, precision, calibration, and product quality of remote-sensing data, leveraging years of multiscale optical system geometric and radiometric calibration and characterization experience. The ECCOE Landsat Cal/Val Team continually monitors the geometric and radiometric performance of active Landsat missions and makes calibration adjustments, as needed, to maintain data quality at the highest level.

This report provides observed geometric and radiometric analysis results for Landsats 7–8 for quarter 1 (January–March), 2022. All data used to compile the Cal/Val analysis results presented in this report are freely available from the USGS EarthExplorer website: https://earthexplorer.usgs.gov.

One specific activity that the Cal/Val Team continued to closely monitor this quarter was the Landsat 8 Thermal Infrared Sensor (TIRS) response degradation, which has been observed since the two November 2020 safehold events. Detailed analysis results characterizing this degradation have been included in this report. Additional information about the safehold events is here: https://www.usgs.gov/core-science-systems/nli/landsat/november-19-2020-landsat-8-data-availability-update-recent-safehold.

Introduction

The U.S. Geological Survey (USGS) Earth Resources Observation and Science (EROS) Calibration and Validation (Cal/Val) Center of Excellence (ECCOE) focuses on improving the accuracy, precision, and quality of remote-sensing data, leveraging years of multiscale optical and thermal system geometric and radiometric calibration and characterization experience (USGS, 2021b). This report provides observed geometric and radiometric analysis results for Landsats 7–8 for quarter 1 (January–March), 2022, and Landsat 8 Thermal Infrared Sensor (TIRS) degradation analysis results from observations since the safehold events in November 2020. Additional information about the safehold events is here: https://www.usgs.gov/core-science-systems/nli/landsat/november-19-2020-landsat-8-data-availability-update-recent-safehold.

Background

The U.S. Department of the Interior is directed to ensure that U.S. land imaging needs are met in the future and to maintain U.S. leadership in civil land imaging and land science. Those directives come in the context of the Future of Land Imaging Interagency Working Group's report titled "A Plan for a U.S. National Land Imaging Program" (Executive Office of the President of the United States, 2007), and two recent Earth Observation (EO) publications (Executive Office of the President of the United States, 2014, 2016). These reports identified Landsat and other key USGS EO assets as critical components in the national EO structure, where several assets were ranked in the top 10 of more than 300 assets. Among them, Landsat ranked third or greater.

Continuity with the past is key to meeting future land imaging science needs. The USGS's currently active Landsat program is the longest continuous record of satellite-based Earth imaging. Landsat data quality is viewed by the remote-sensing user community as a gold standard (National Geospatial Advisory Committee, 2020).

To ensure the continued excellent quality of Landsat data, the USGS EROS Center has identified maintaining a well-calibrated long-term remote-sensing archive for science, and developing and understanding land remote-sensing requirements and land imaging solutions, as key strategic pillars. Understanding the land imaging requirements of current and future users—along with an ability to assess the capabilities of

[1]KBR, Inc.; Work done under contract to the U.S. Geological Survey.

[2]U.S. Geological Survey.

[3]National Aeronautics and Space Administration.

[4]Science Systems and Applications, Inc.; Work done under contract to the National Aeronautics and Space Administration.

current and future systems for meeting those requirements—is also key to meeting future land imaging science needs. In the past, Cal/Val activities at the EROS Center addressing the above pillars were spread across multiple groups. The USGS EROS Center strategically brought the multiple groups together and formed a single team in a unified project called the ECCOE to enable the USGS to more efficiently address national and global land remote-sensing needs.

Purpose and Scope

The primary purpose of this report is to provide the latest geometric and radiometric performance results for all active Landsat missions. All data used to compile the results presented in this report are available from the USGS EarthExplorer website: https://earthexplorer.usgs.gov (USGS, 2021a).

Processing Level Definitions

This report frequently references Landsat processing levels. A description of these processing levels are in the subsections below.

Level 0

The Level 0 Reformatted Archive (L0Ra) and Level 0 Reformatted Product (L0Rp) formats do not have sensor chip assembly or band alignment performed. L0Ra data are sensor data and spacecraft ancillary data that are reformatted for easier processing. Minor corrections to the ancillary data are performed (such as frame number and time-code corrections), and ancillary raw data units are converted to engineering units. Image data are left in counts or digital numbers. L0Rp and L0Ra files are in the same format, but the content is different. L0Ra files contain an entire interval of imagery, whereas L0Rp files only contain a smaller part of that L0Ra data: a Worldwide Reference System–2 (WRS–2) scene-based subset.

Level 1

The standard Level 1 (L1) image data are radiometrically and geometrically corrected. L1 Geometric Systematic Correction products are radiometrically calibrated with only systematic geometric corrections applied using the spacecraft ephemeris data. L1 Systematic Terrain Correction products are radiometrically calibrated with systematic geometric corrections applied using the spacecraft ephemeris data and digital elevation model data to correct for relief displacement. L1 Terrain Precision Correction (L1TP) products are radiometrically calibrated and orthorectified using ground control points (GCPs) and digital elevation model data to correct for relief displacement.

Level 2

The Level 2 science products are generated from L1 inputs that meet the less than 76-degree solar zenith angle constraint and include the required auxiliary data inputs to generate a scientifically viable product. Level 2 science products represent surface reflectance and surface temperature. Surface reflectance is the fraction of incoming solar radiation that is reflected from the Earth's surface. Surface reflectance product generation accounts for the temporally, spatially, and spectrally varying scattering and absorbing effects of atmospheric gases, aerosols, and water vapor, which are necessary to reliably characterize the Earth's land surface.

Surface temperature is the measurement of the temperature of the surface of the Earth in Kelvin (K). Provisional surface temperature is generated from the Landsat Collection 2 L1 thermal infrared bands, top of atmosphere reflectance, Advanced Spaceborne Thermal Emission and Reflection Radiometer (ASTER) Global Emissivity Database data, ASTER Normalized Difference Vegetation Index data, and atmospheric profiles of geopotential height, specific humidity, and air temperature extracted from reanalysis data.

Landsat Collection Definitions

This report frequently references Landsat collections. In 2016, the USGS reorganized the Landsat archive into a tiered-collection management structure. This structure ensures that all Landsat L1 products provide a consistent archive of known data quality while controlling continuous improvement of the archive and access to all data as they are acquired. The implementation of collections represents a substantial change in the management of the Landsat archive by ensuring consistent quality over time and across all instruments.

Landsat Collection 1

Landsat Collection 1 was released in 2016 and introduced collection tiers for L1 data products based on data quality and the level of processing. The tier definition purpose was to support easier identification of suitable scenes for time-series pixel-level analysis. In addition to tiered products, several additional changes were first introduced with the release of Collection 1 processing. Because of the release of Landsat Collection 2 in December 2020, Collection 1 processing of newly acquired data ended on January 1, 2022. Access to archived Collection 1 data products are planned to cease in late 2022. Additional information about the Collection 1 products is here: https://www.usgs.gov/core-science-systems/nli/landsat/landsat-collection-1.

Landsat Collection 2

Landsat Collection 2 was released in December 2020 and marked the second major reprocessing effort on the Landsat archive (USGS, 2020a, 2020b). Collection 2 represented several data product improvements that harnessed recent advancements in data processing, algorithm development, and data access and distribution capabilities. Additional information about the Collection 2 products is here: https://www.usgs.gov/core-science-systems/nli/landsat/landsat-collection-2.

Landsat 8 Radiometric Performance Summary

Radiometric Performance Summary

The Landsat 8 on-orbit radiometric performance for this reporting quarter (quarter 1, January–March 2022) meets all requirements as outlined in USGS (2019b). The quarterly Operational Land Imager (OLI) and Thermal Infrared Sensor (TIRS) radiometric performance summaries are provided in tables 1 and 2, respectively.

Operational Land Imager Signal-to-Noise Ratio

The signal-to-noise ratio (SNR) for each of the OLI spectral bands is characterized at a prescribed band-specific typical radiance ($L_{typical}$) level, as described in table 3. The SNR of a detector at a given radiance level is defined as the mean of the measured pixel radiances acquired over a homogenous target divided by their standard deviation. A curve is fit to the SNR at the measured radiance levels and is evaluated at the prescribed $L_{typical}$. The SNR is characterized at multiple stages of the instrument build, culminating in the testing of the fully integrated instrument.

OLI SNR is evaluated on orbit each month. It remains consistently 2–3 times better than requirements and about 8 times better than Landsat 7 Enhanced Thematic Mapper Plus (ETM+) SNR. Collection 2 SNR slightly increased because of improvement in the bias calculation, further exceeding requirement thresholds. Figure 1 shows per-band OLI median SNR at $L_{typical}$ (yellow bars) for March 2022, which for all bands easily exceed the OLI SNR requirements (blue bars) by more than 50 percent. Lifetime SNR stability at $L_{typical}$ for each OLI band is represented in figures 2, 3, 4, 5, 6, 7, 8, 9, and 10; monthly SNR values (for the detectors that have median SNRs for all bands) are denoted by the diamonds, and the uncertainties in the monthly SNR model are denoted by the error bars.

Table 1. Landsat 8 Operational Land Imager radiometric performance summary, quarter 1, 2022.

[The previous quarter is quarter 4, 2021. OLI, Operational Land Imager; <, less than; SNR, signal-to-noise ratio; $L_{typical}$, typical radiance; -, not applicable; L_{high}, high radiance; RMS, root mean square; stdev, standard deviation; ≤, less than or equal to; W/m² sr µm, watt per square meter per steradian per micrometer; σ, sigma; spec, specification]

Requirement	Measured value from this quarter	Measured value from previous quarter	Required value	Unit
OLI ghosting	Meets	Meets	Varies	Percent
OLI absolute radiance uncertainty	4	4	<5	Percent
OLI absolute reflectance uncertainty	<3	<3	<3	Percent
OLI median SNR $L_{typical}$	Meets	Meets	Varies	-
OLI median SNR L_{high}	Meets	Meets	Varies	-
OLI uniformity full field of view	0.35	0.35	<0.5	Percent
OLI uniformity banding RMS	0.80	0.80	<1	Percent
OLI uniformity banding stdev	0.15	0.15	<0.25	Percent
OLI uniformity streaking	0.5	0.5	≤0.5, 1	Percent
OLI coherent noise	Meets	Meets	Less than coherent noise threshold curve	-
OLI saturation radiances	Meets	Meets	Varies	W/m² sr µm
OLI 16-day radiometric stability	0.12	0.12	<1	Percent (2σ)
OLI 60-second radiometric stability	0.1	0.1	<0.5	Percent (2σ)
OLI inoperable detectors	0	0	<0.1	Percent
OLI out-of-spec detectors	0.06	0.06	<0.25	Percent

Table 2. Landsat 8 Thermal Infrared Sensor radiometric performance summary, quarter 1, 2022.

[The previous quarter is quarter 4, 2021. TIRS, Thermal Infrared Sensor; ~, approximately; NEΔT, noise equivalent delta temperature; K, Kelvin; TBD, to be determined; RMS, root mean square; stdev, standard deviation; <, less than; -, not applicable; W/m² sr µm, watt per square meter per steradian per micrometer; σ, sigma; spec, specification]

Requirement	Measured value from this quarter	Measured value from previous quarter	Required value	Unit
TIRS absolute radiance uncertainty	~1	~1	<2	Percent
TIRS NEΔT (at 300K)	0.05	0.05	<0.4	K
TIRS uniformity full field of view	TBD	TBD	<0.5	Percent
TIRS uniformity banding RMS	TBD	TBD	<0.5	Percent
TIRS uniformity banding stdev	TBD	TBD	<0.5	Percent
TIRS uniformity streaking	<0.5	<0.5	<0.5	Percent
TIRS coherent noise	Meets	Meets	Less than coherent noise threshold curve	-
TIRS saturation radiances	28.4, 19.2	28.4, 19.2	>20.5, >17.8	W/m² sr µm
TIRS 40-minute radiometric stability	0.1	0.1	<0.7	Percent (1σ)
TIRS inoperable detectors	0	0	<0.1	Percent
TIRS out-of-spec detectors	0.21	0.21	<0.25	Percent

Table 3. Landsat 8 Operational Land Imager typical radiances for each spectral band.

[OLI, Operational Land Imager; nm, nanometer; $L_{typical}$, typical radiance; W/m² sr µm, watt per square meter per steradian per micrometer]

OLI band number	Spectral band	Center wavelength (nm)	$L_{typical}$ (W/m² sr µm)
1	Coastal/aerosol	443	40
2	Blue	482	40
3	Green	561	30
4	Red	655	22
5	Near infrared	865	14
6	Shortwave infrared 1	1,609	4.0
7	Shortwave infrared 2	2,201	1.7
8	Panchromatic	590	23
9	Cirrus	1,373	6.0

SNR for each band has remained very stable over time (within the uncertainty of the models and well above the required levels).

Thermal Infrared Sensor Noise Performance

Noise can be defined as variation in detected signal over time when observing a stable source of radiation. For thermal sensors, noise is usually expressed in terms of a change in brightness temperature (that is, the noise equivalent change in temperature [NEΔT]). NEΔT is estimated as the standard deviation of detector data acquired over a uniform radiance source and then converted to temperature. Noise performance is conducted on blackbody and deep space TIRS data (Montanaro and others, 2014).

All TIRS detectors have similar NEΔT. At 300K, band average noise performance for both thermal bands is about eight times better than requirement (less than 0.4K) and about four times better than the NEΔT of the Landsat 7 ETM+ thermal band at that same temperature. Figure 11 shows lifetime averages of NEΔT at 300K for TIRS band 10, and figure 12 shows the same averages for TIRS band 11. In both figures, colored diamonds are used to indicate the observed NEΔT values as measured over time.

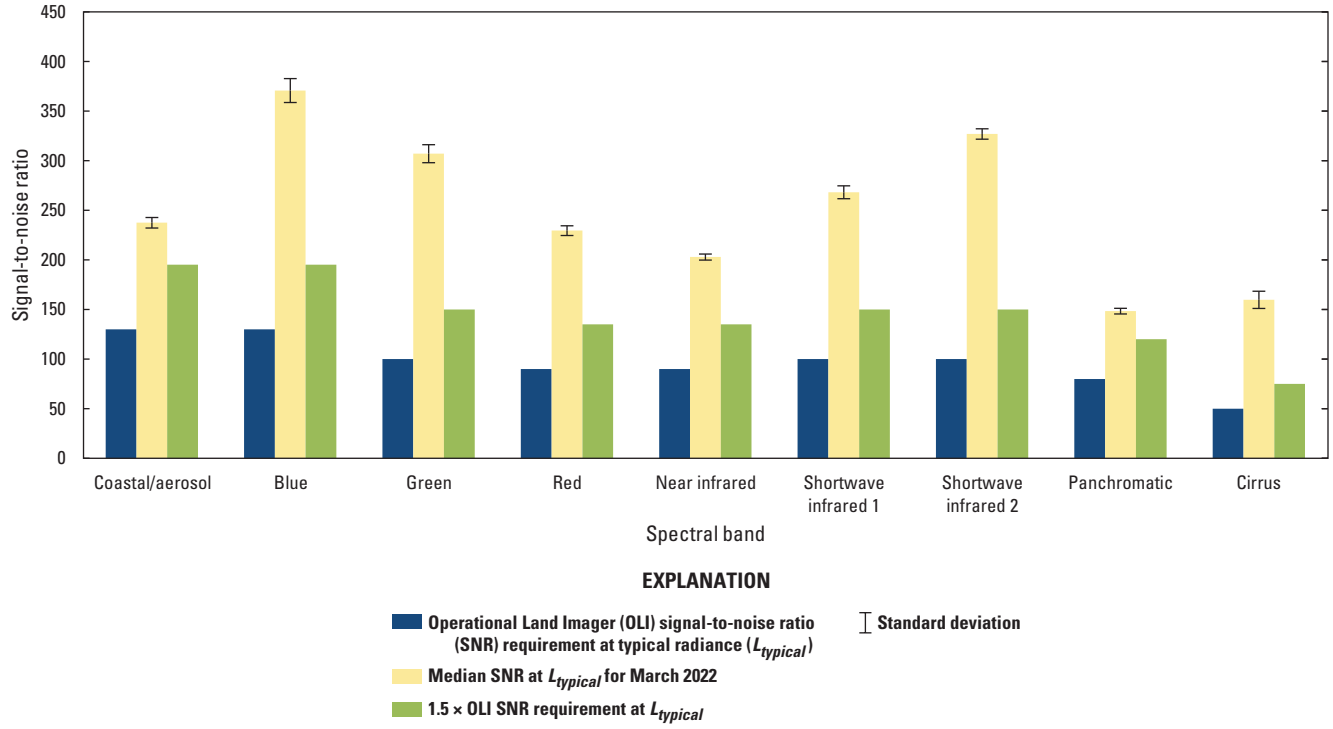

Figure 1. Landsat 8 Operational Land Imager signal-to-noise performance, March 2022.

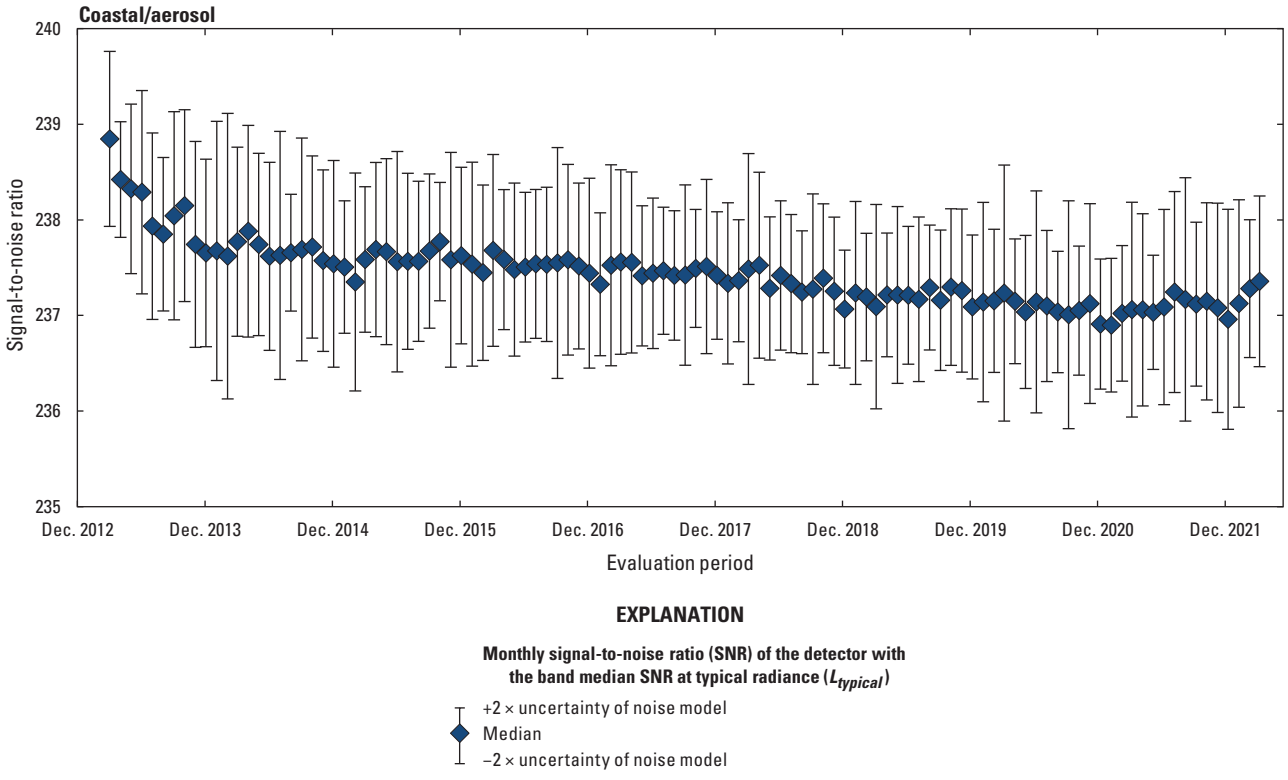

Figure 2. Landsat 8 Operational Land Imager coastal/aerosol band lifetime signal-to-noise ratio stability.

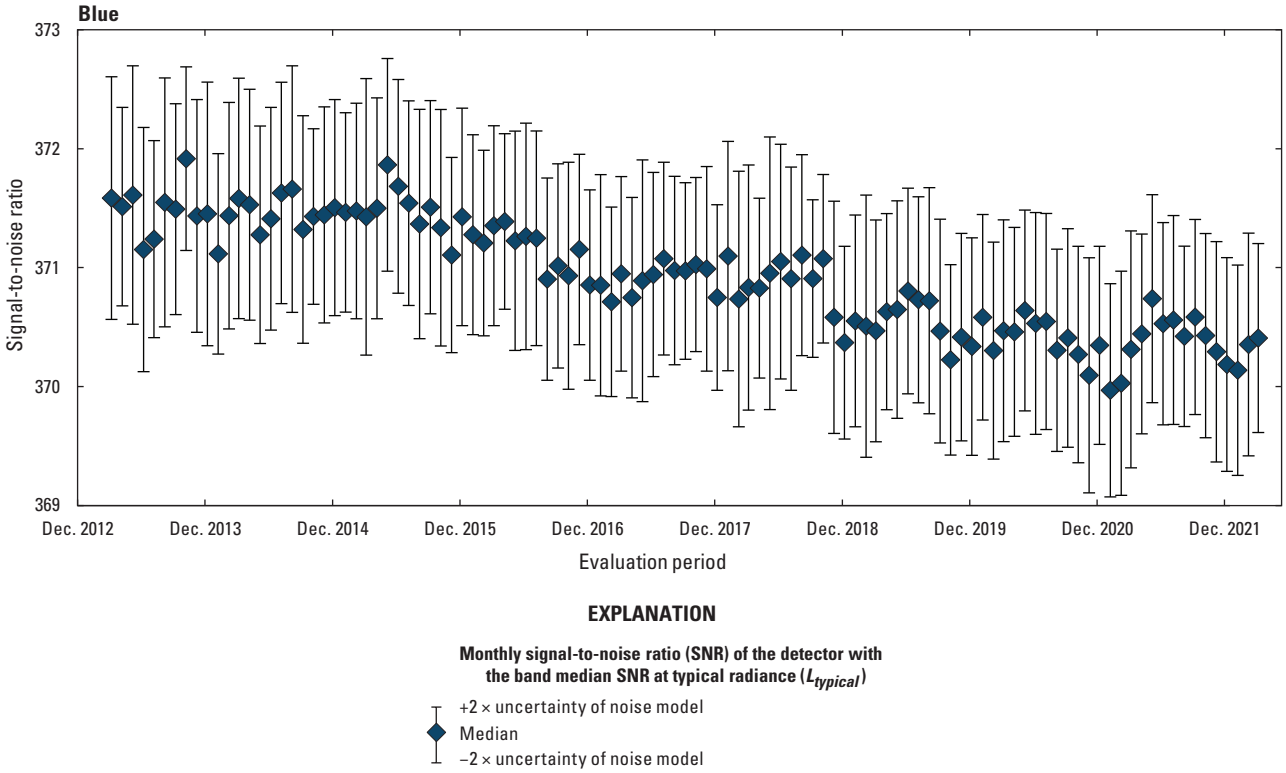

Figure 3. Landsat 8 Operational Land Imager blue band lifetime signal-to-noise ratio stability.

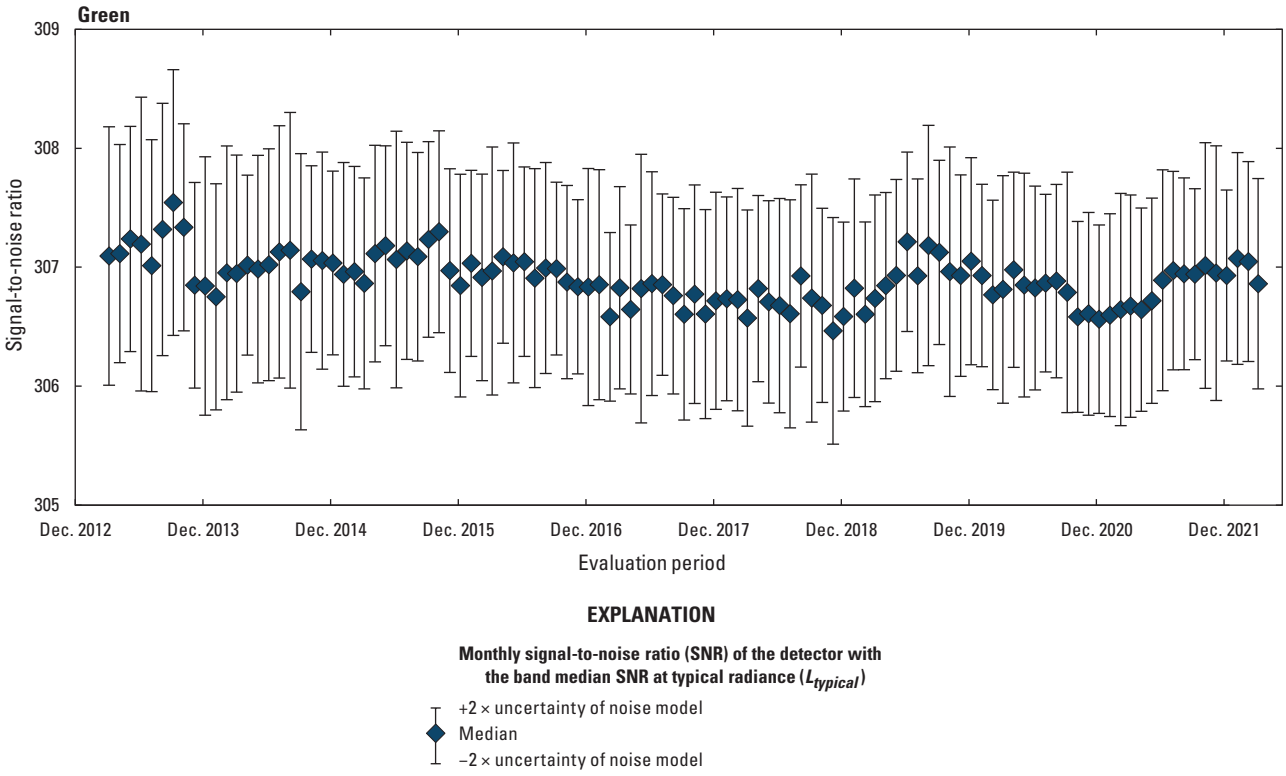

Figure 4. Landsat 8 Operational Land Imager green band lifetime signal-to-noise ratio stability.

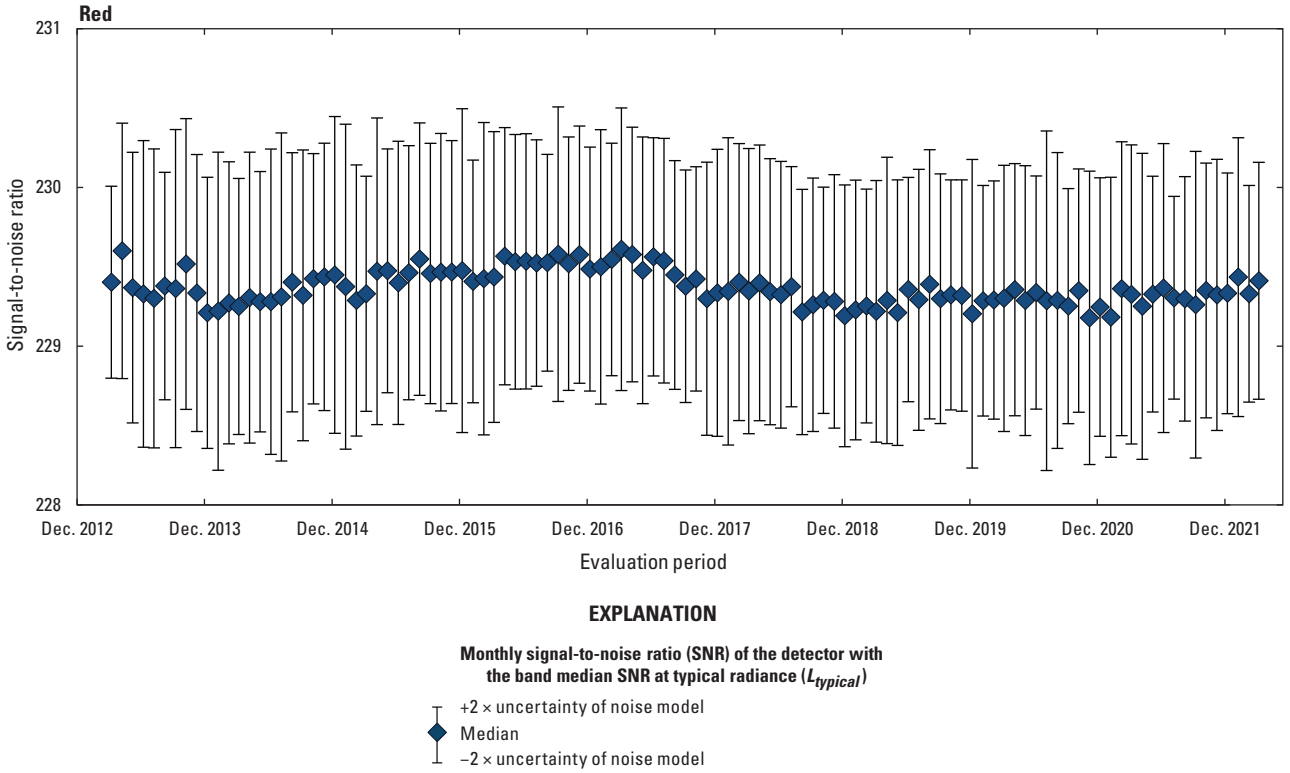

Figure 5. Landsat 8 Operational Land Imager red band lifetime signal-to-noise ratio stability.

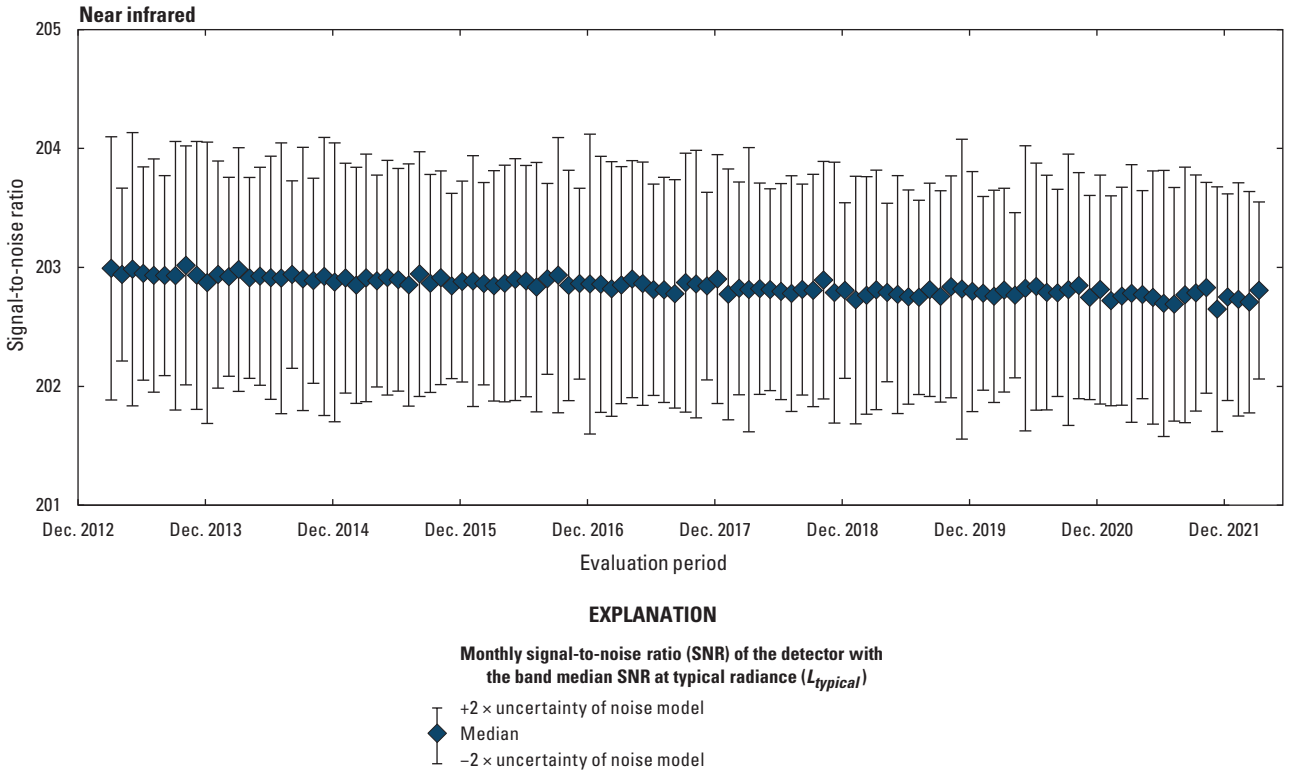

Figure 6. Landsat 8 Operational Land Imager near infrared band lifetime signal-to-noise ratio stability.

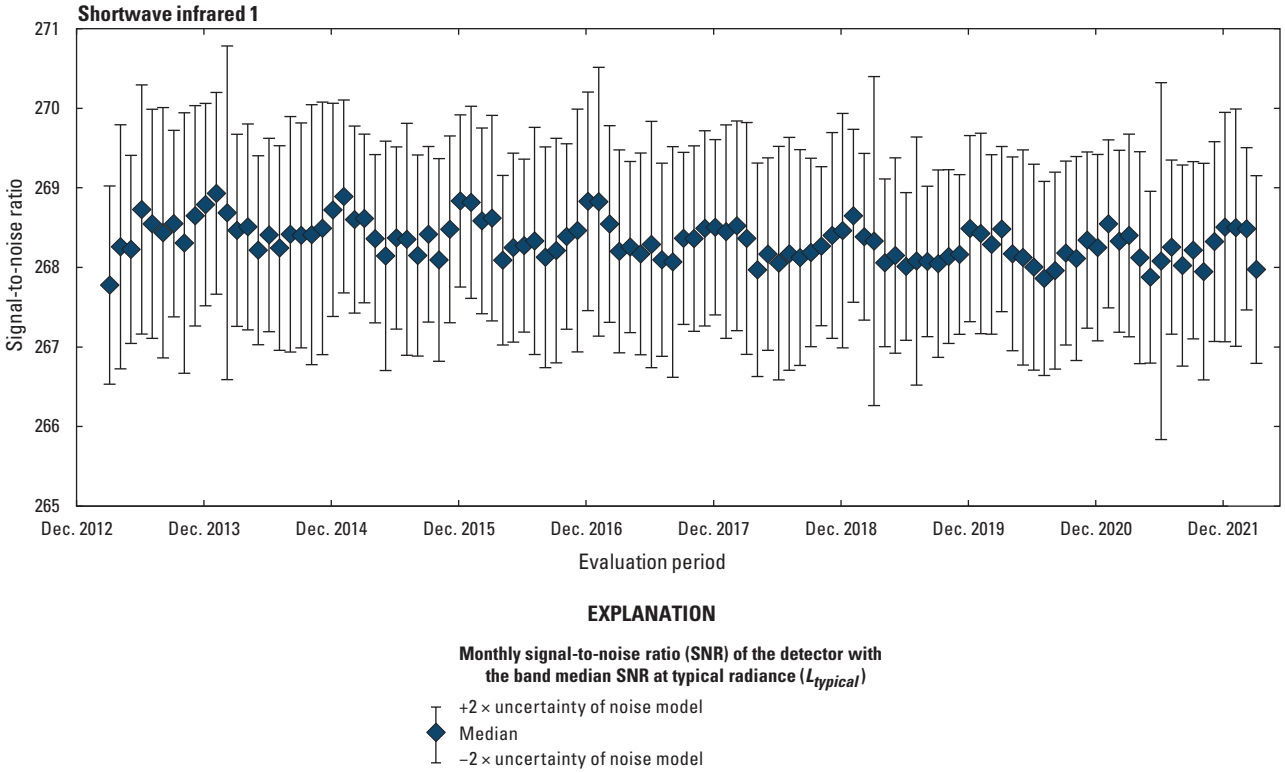

Figure 7. Landsat 8 Operational Land Imager shortwave infrared 1 band lifetime signal-to-noise ratio stability.

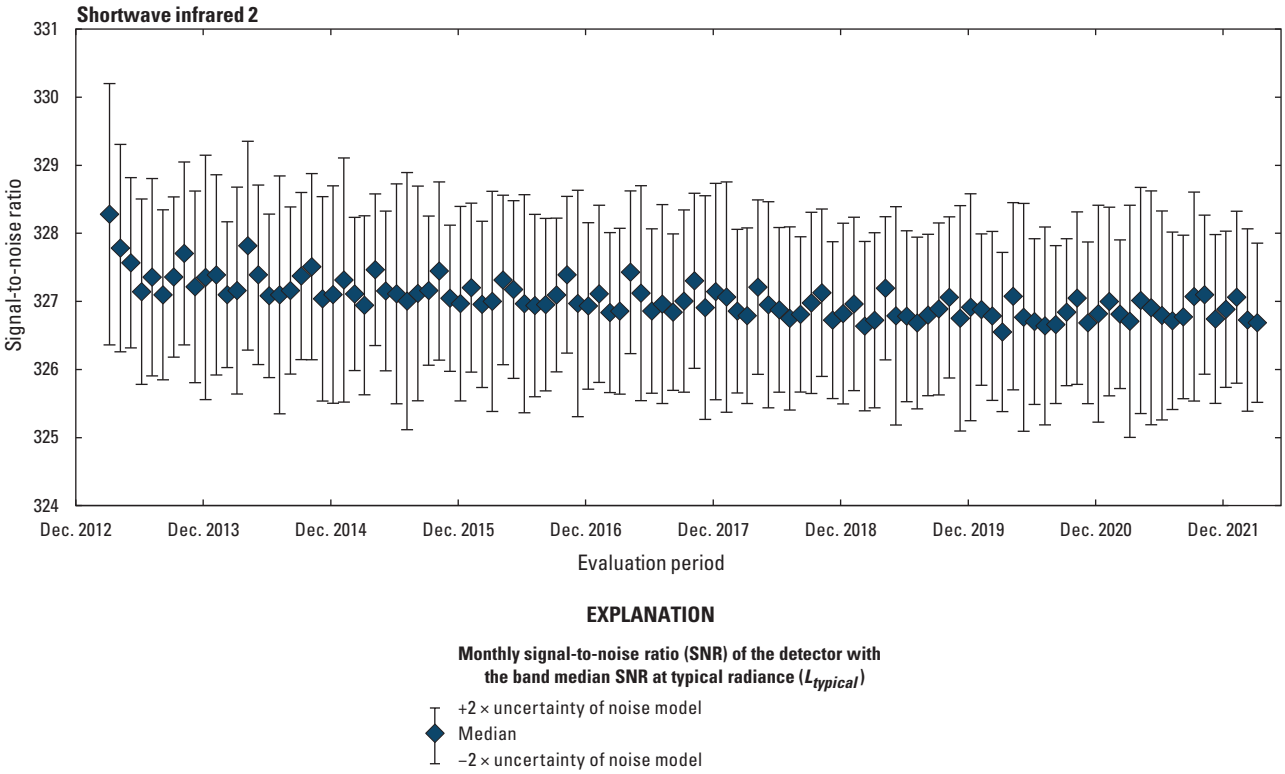

Figure 8. Landsat 8 Operational Land Imager shortwave infrared 2 band lifetime signal-to-noise ratio stability.

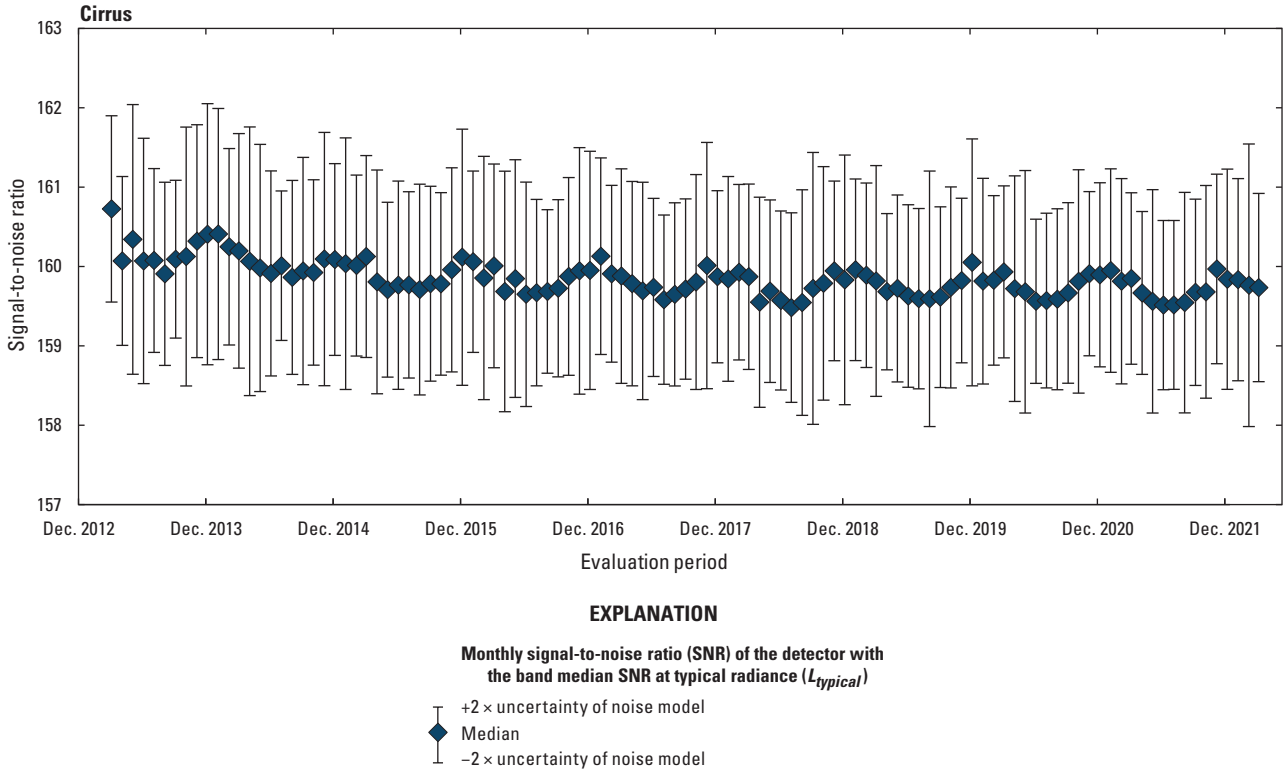

Figure 9. Landsat 8 Operational Land Imager cirrus band lifetime signal-to-noise ratio stability.

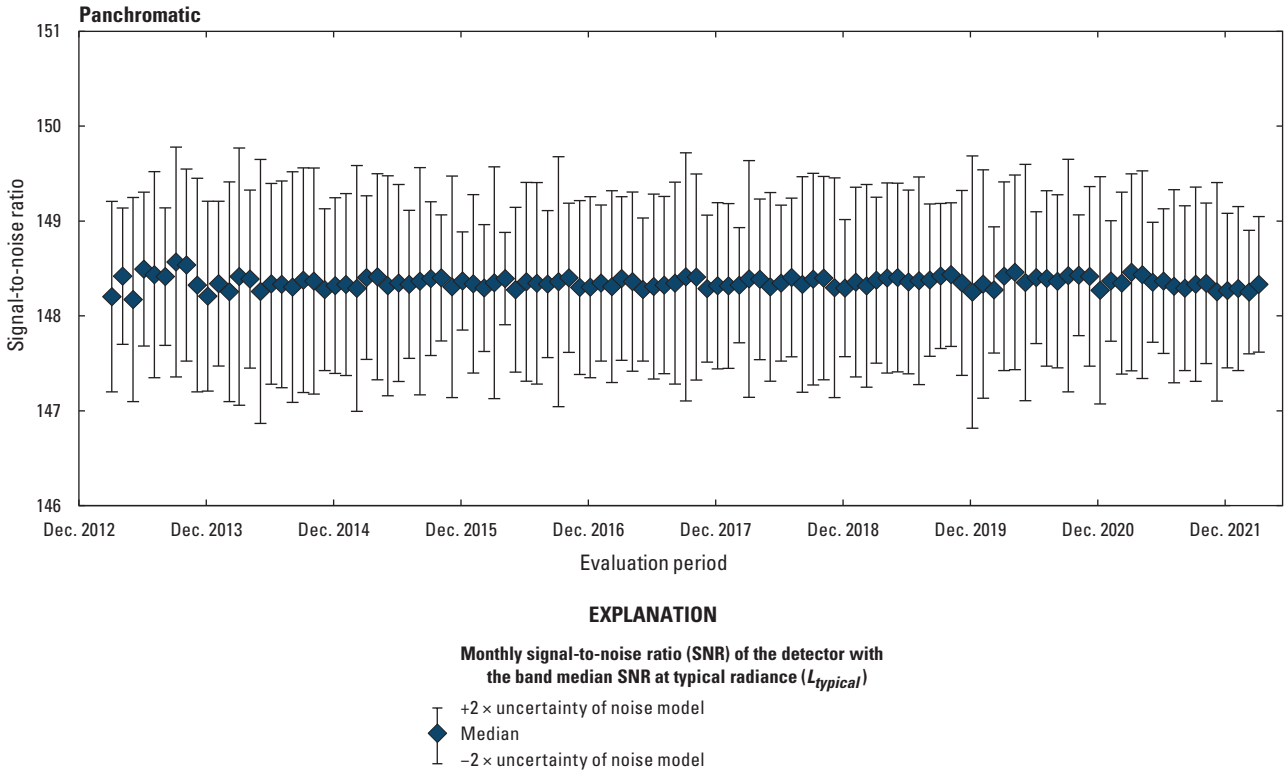

Figure 10. Landsat 8 Operational Land Imager panchromatic band lifetime signal-to-noise ratio stability.

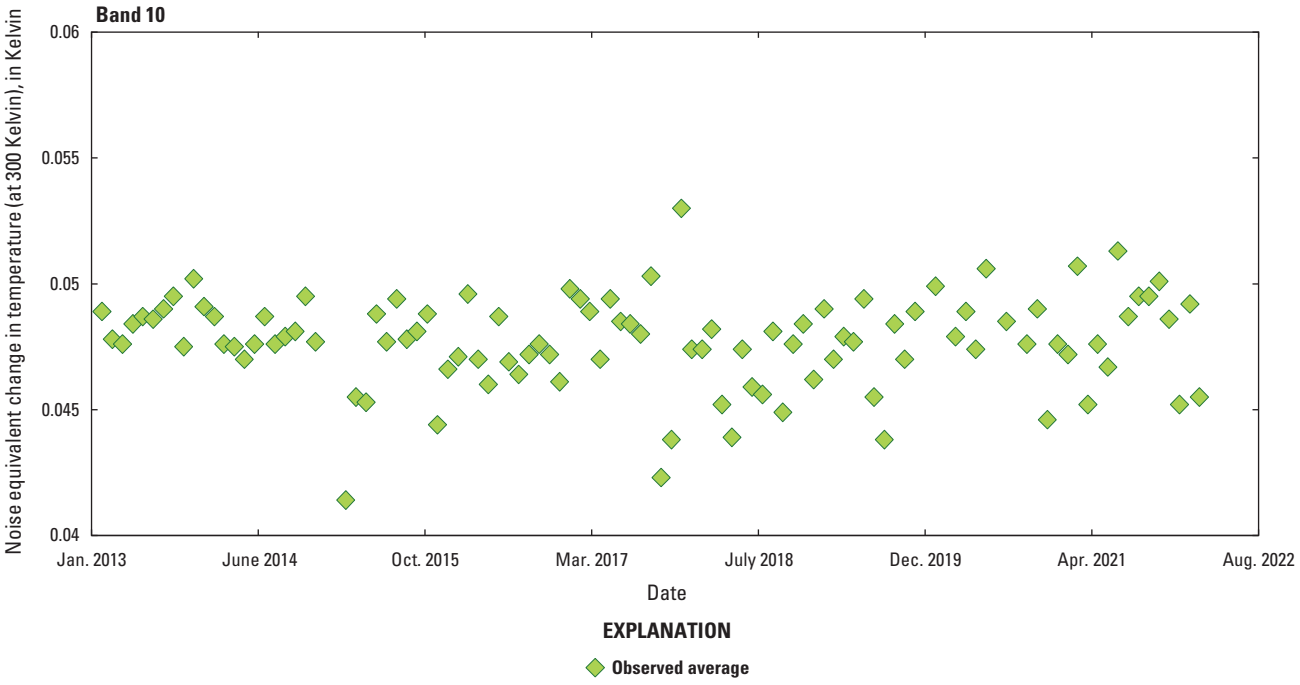

Figure 11. Landsat 8 Thermal Infrared Sensor band 10 lifetime noise performance.

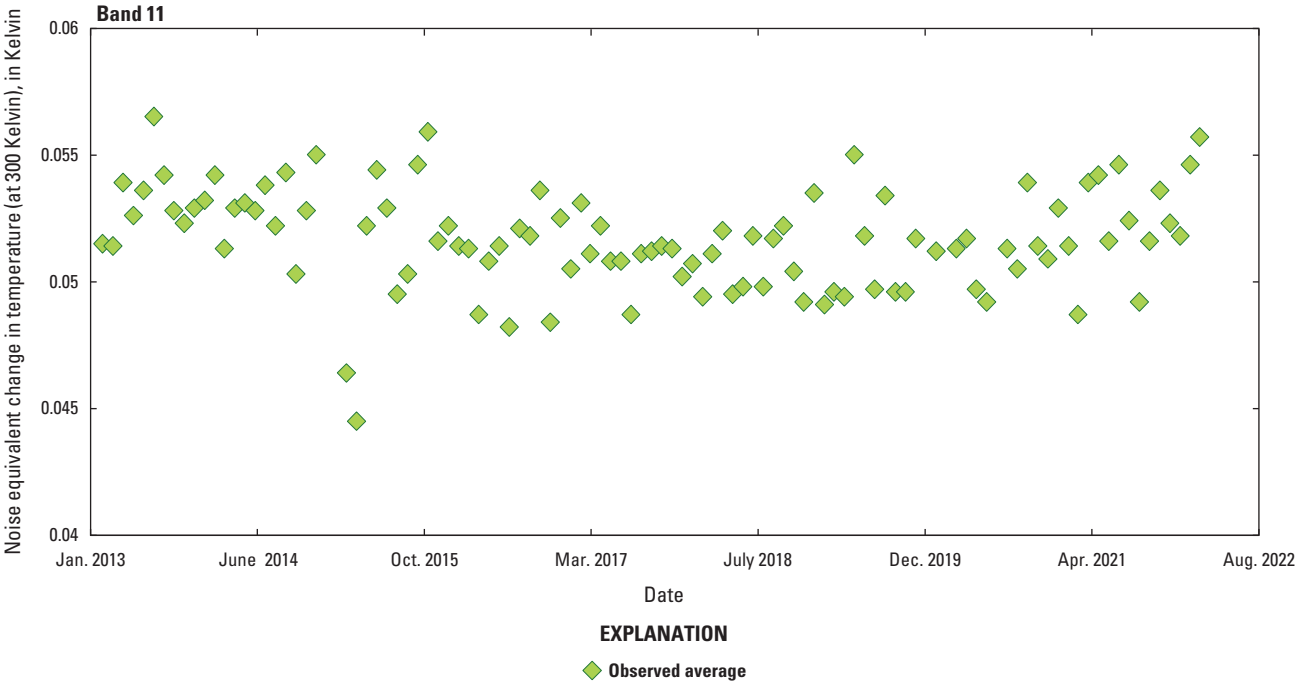

Figure 12. Landsat 8 Thermal Infrared Sensor band 11 lifetime noise performance.

Radiometric Stability

Radiometric stability of an instrument is fundamental to low uncertainty in the radiometric calibration of data products generated from its measurements. The radiometric response stability is characterized for all OLI and TIRS bands using the instruments' responses to signals from the on-board calibration devices collected over time (USGS, 2021d). The bias and gain stability of an instrument are contributing factors to variability within a radiometrically calibrated product.

Figures 13, 14, 15, 16, 17, 18, 19, 20, and 21 show per-band OLI radiometric stability over the lifetime of the instrument. Within each figure, the x-axis represents years since launch (February 11, 2013) and the y-axis represents the response relative to mission day 75. The solid green line on figures 13 and 14 represents the gain model used over time, which is derived from the OLI response to the stimulation lamps, solar panels, and lunar collects; it is only shown for the bands with responsivity (gain) determined to be slowly changing over time (coastal/aerosol and blue bands). For the remaining bands, response changes were minuscule until the safehold events in November 2020. These observations indicate high radiometric stability of the instrument over its lifetime. Data derived from bands that have changed responsivity are corrected during product generation, so final products are not affected.

Figures 22 and 23 show the long-term stability of the TIRS side A electronics that were used for the first approximately (~) 700 days of the mission. During that period, TIRS gains changed by about 0.2 and 0.1 percent per year for bands 10 and 11, respectively. These trends reduced on the side B electronics to about 0.05 and 0.01 percent until the two safehold events in November 2020, as seen in figures 24 and 25, respectively. After the safehold events, TIRS responsivity has gradually decreased ~3.0 percent for band 10 and ~6.0 percent for band 11. Note that the response degradation is modeled and corrected to within 0.5-percent uncertainty in the L1 products.

Since January 2021, TIRS on-board calibrator acquisitions have been collected on a weekly basis (instead of once every ~2 weeks) to better monitor the degradation in response observed after the safehold events. Weekly calibration acquisitions are planned into the future as long as the response degradation trend continues, and as long as geometric and radiometric accuracies are not negatively affected by the increased acquisition frequency.

Updates to Absolute Radiometric Calibration

Absolute radiometric calibration is established on the ground before launch and transferred to orbit using the solar diffuser for OLI and the blackbody for TIRS. Onboard calibrators and pseudo-invariant calibration sites (PICS; Committee

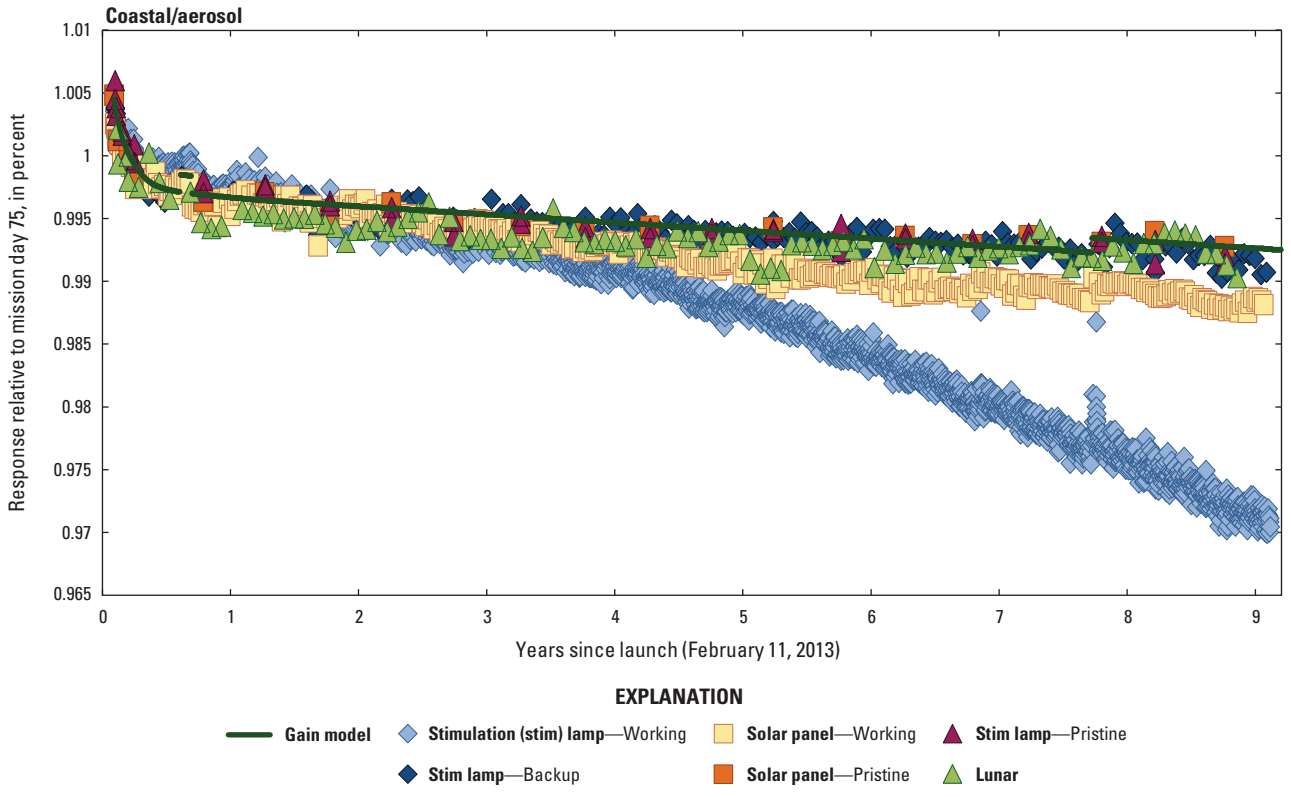

Figure 13. Landsat 8 Operational Land Imager coastal/aerosol band lifetime radiometric stability.

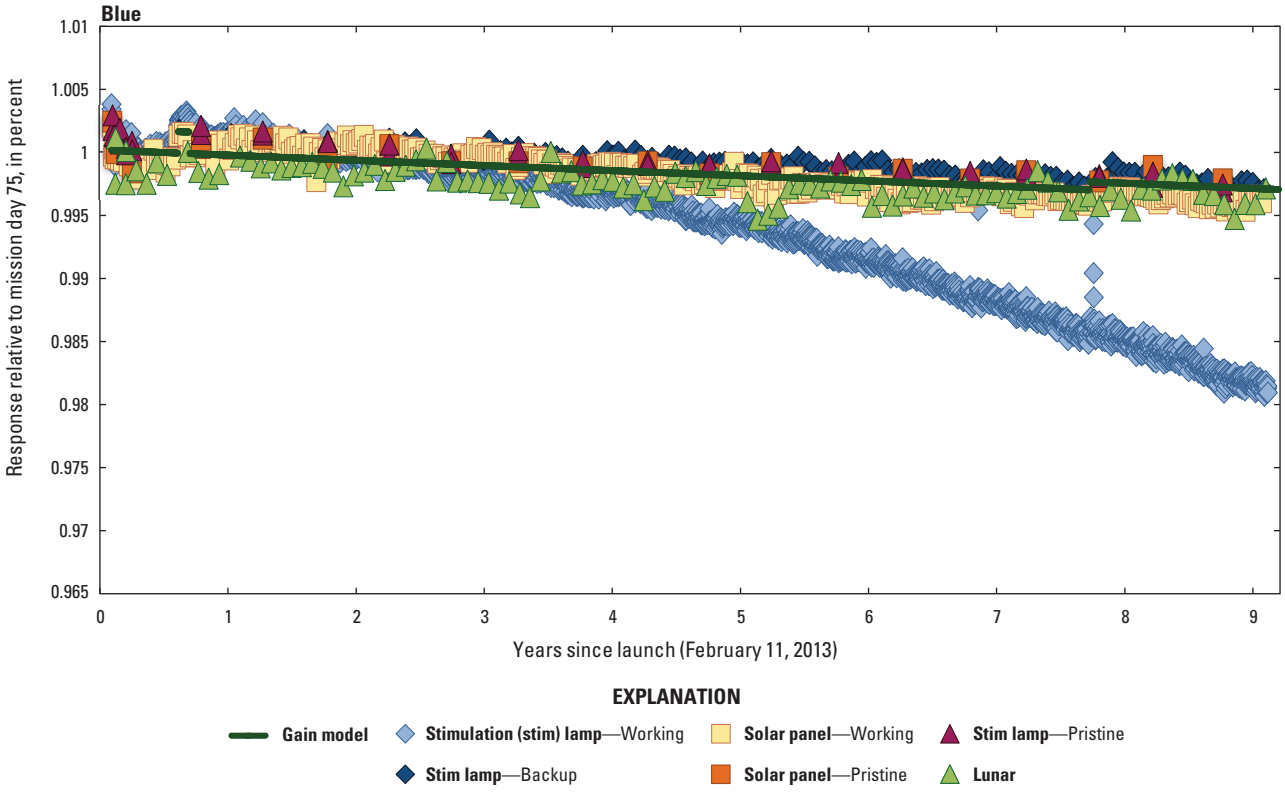

Figure 14. Landsat 8 Operational Land Imager blue band lifetime radiometric stability.

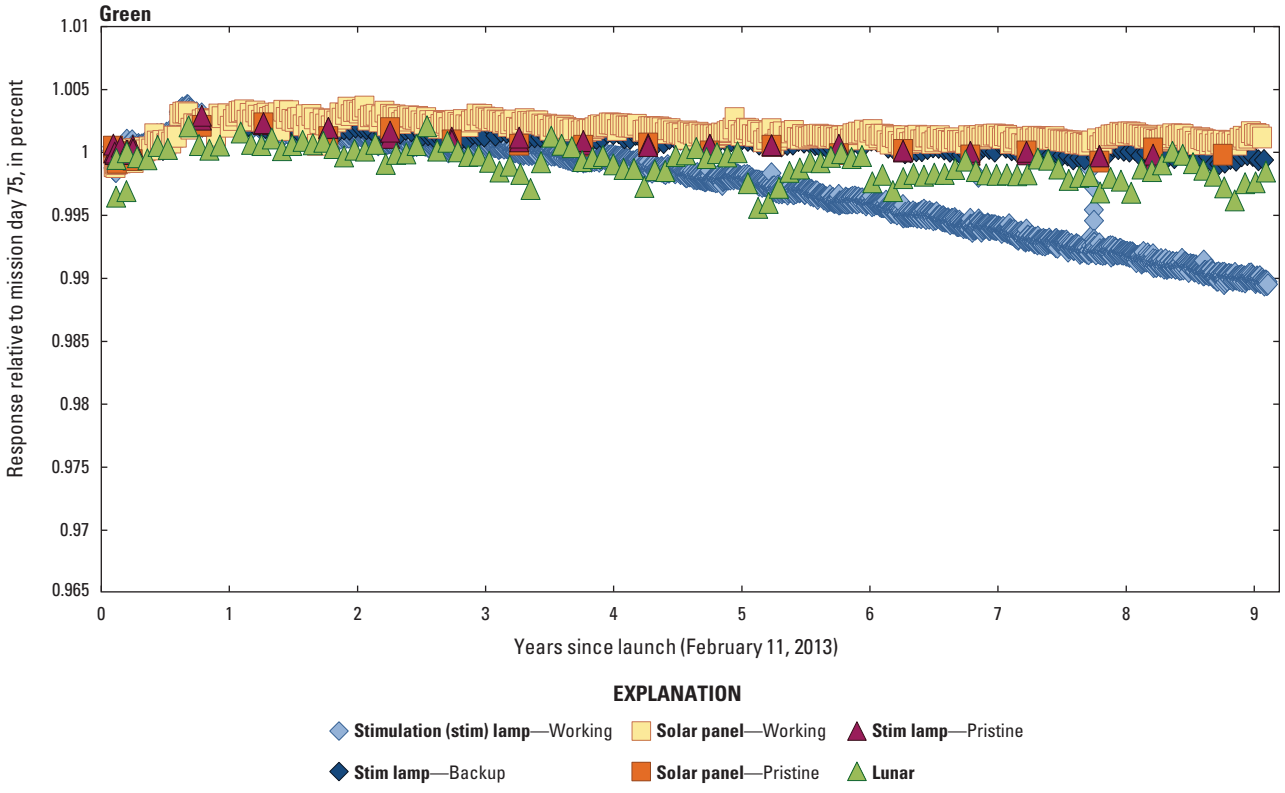

Figure 15. Landsat 8 Operational Land Imager green band lifetime radiometric stability.

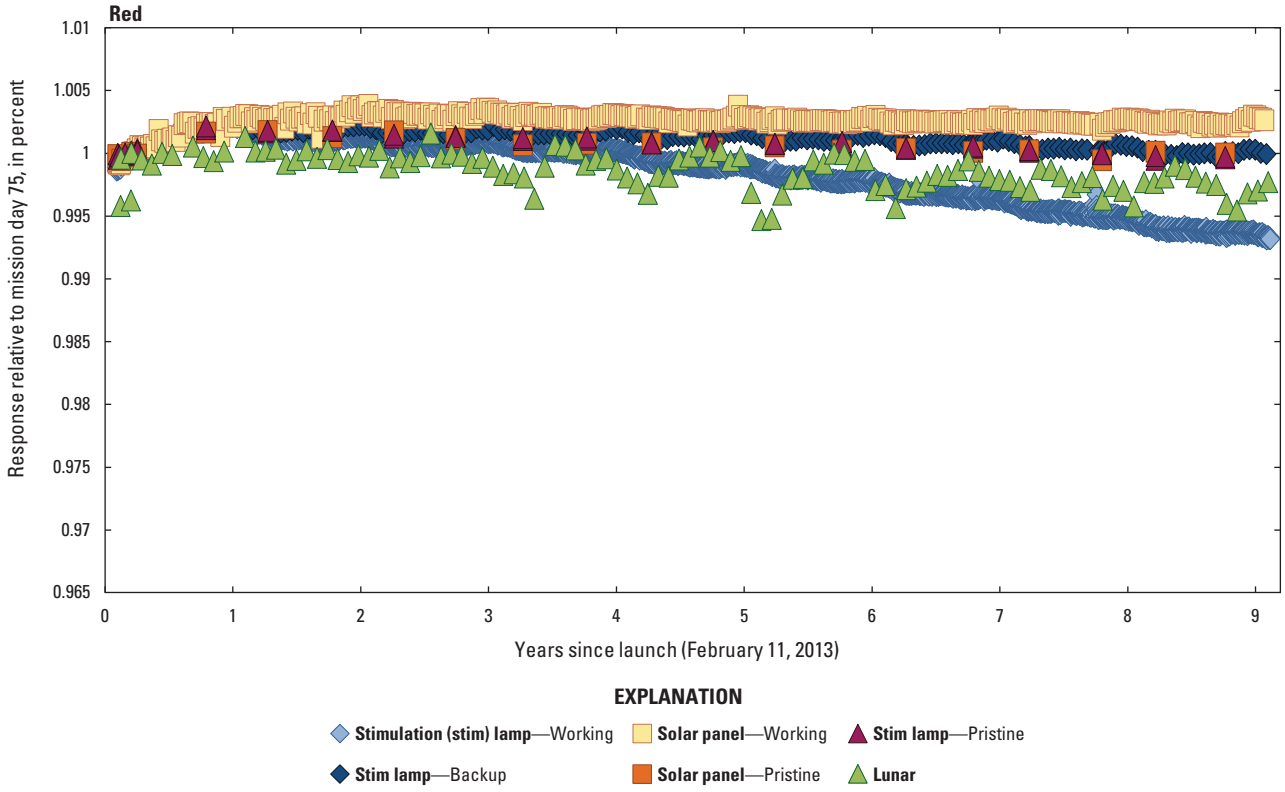

Figure 16. Landsat 8 Operational Land Imager red band lifetime radiometric stability.

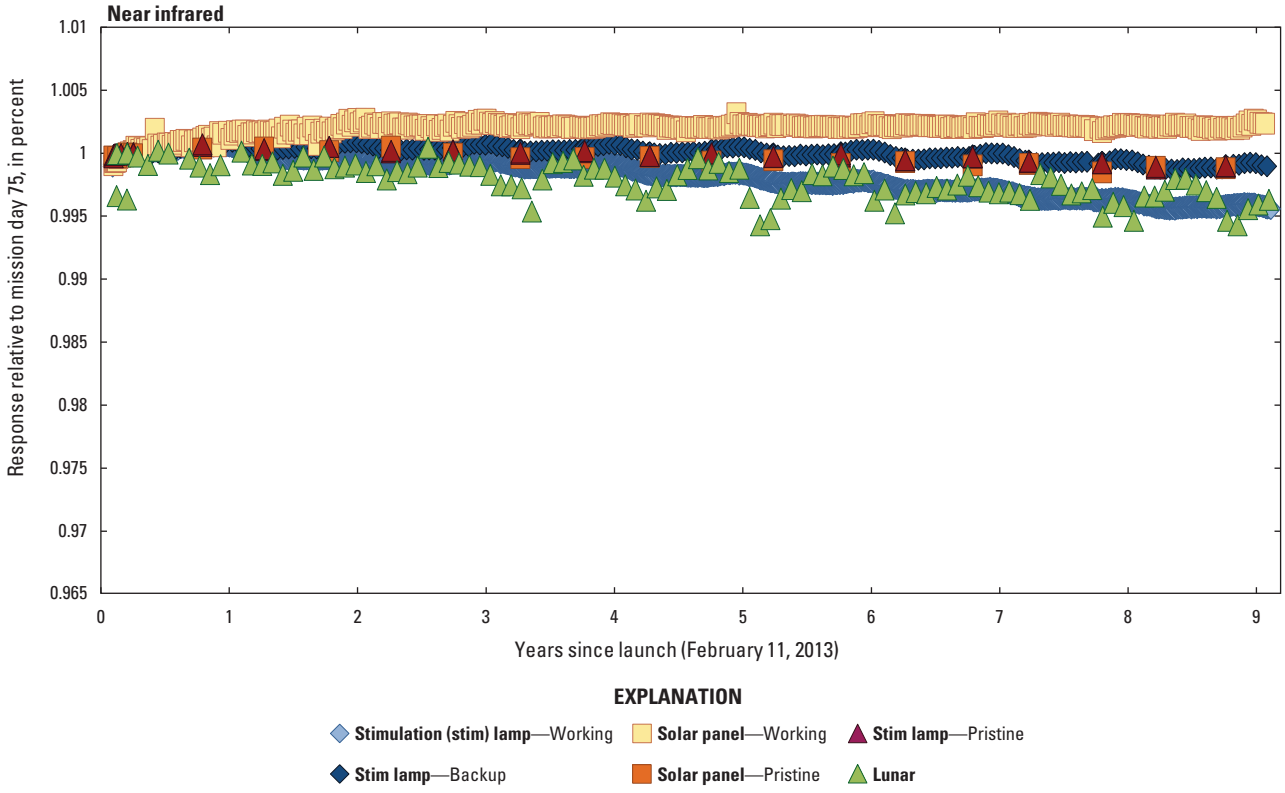

Figure 17. Landsat 8 Operational Land Imager near infrared band lifetime radiometric stability.

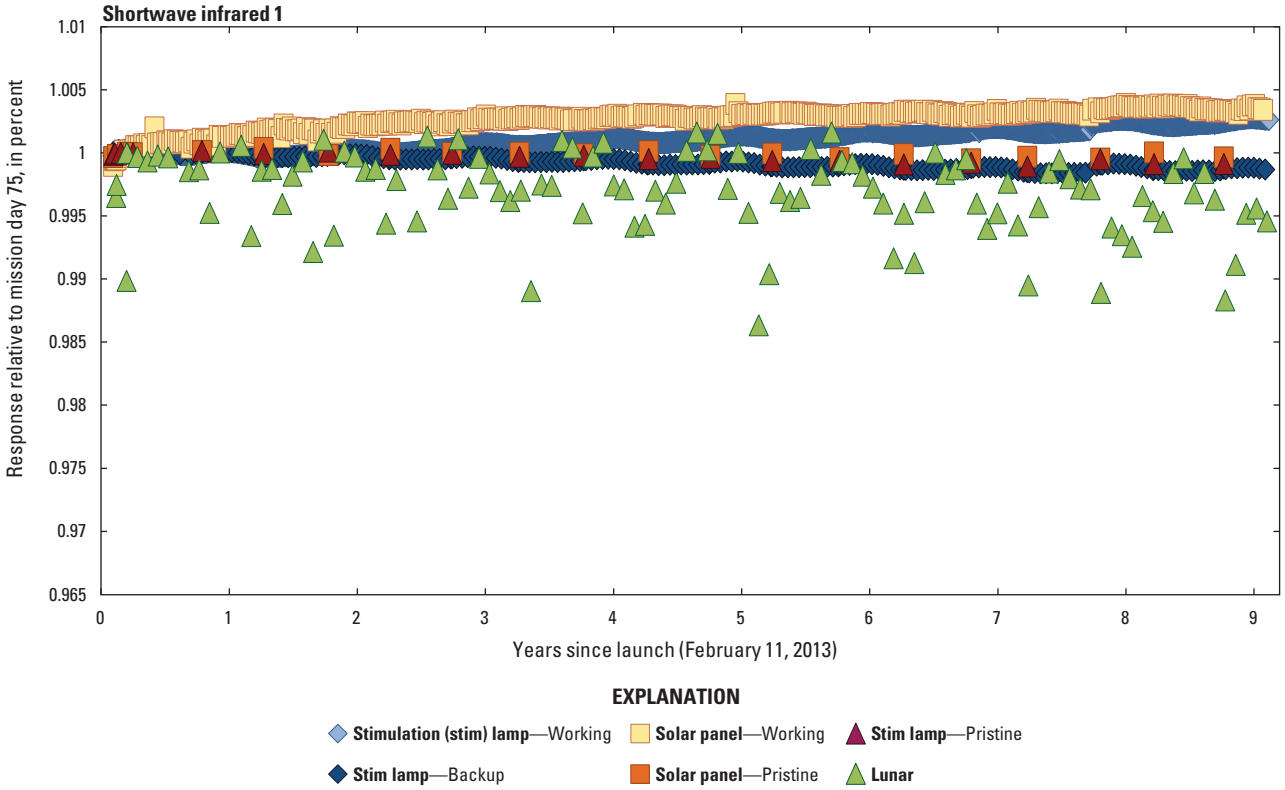

Figure 18. Landsat 8 Operational Land Imager shortwave infrared 1 band lifetime radiometric stability.

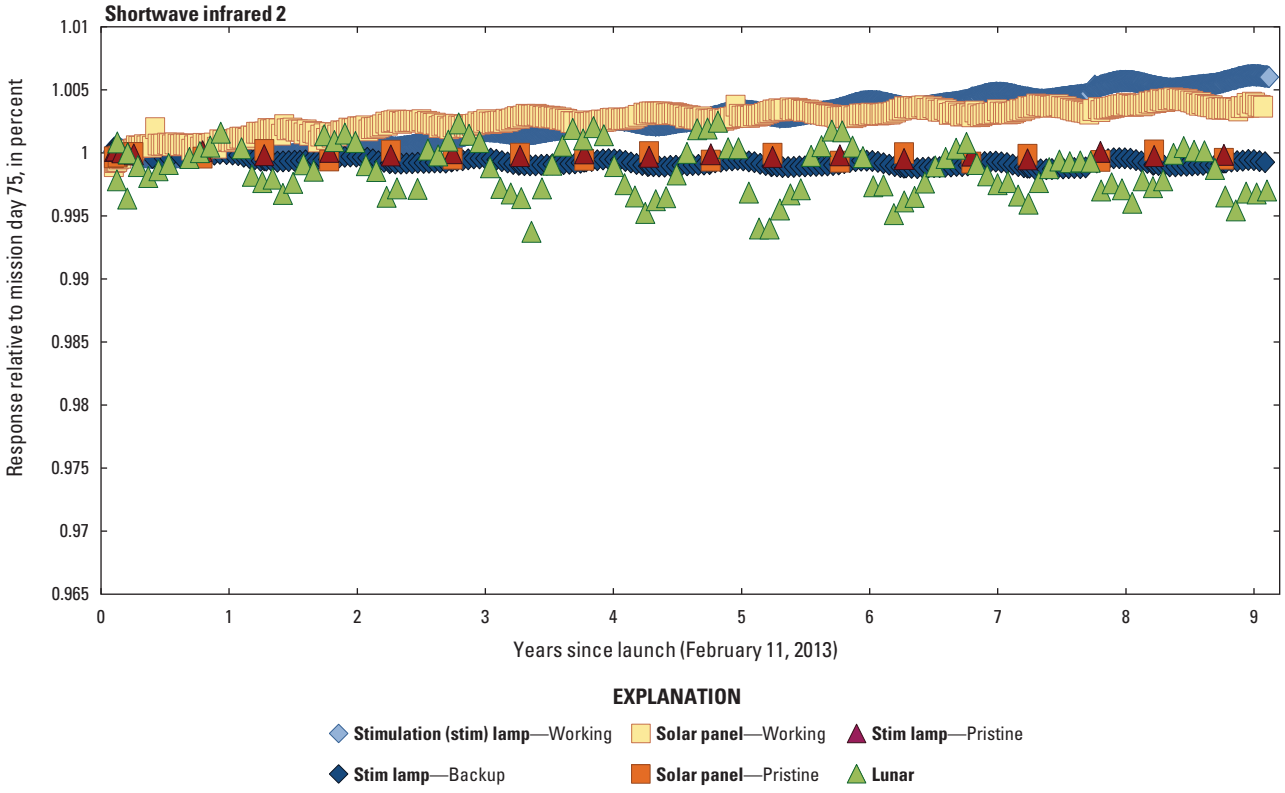

Figure 19. Landsat 8 Operational Land Imager shortwave infrared 2 band lifetime radiometric stability.

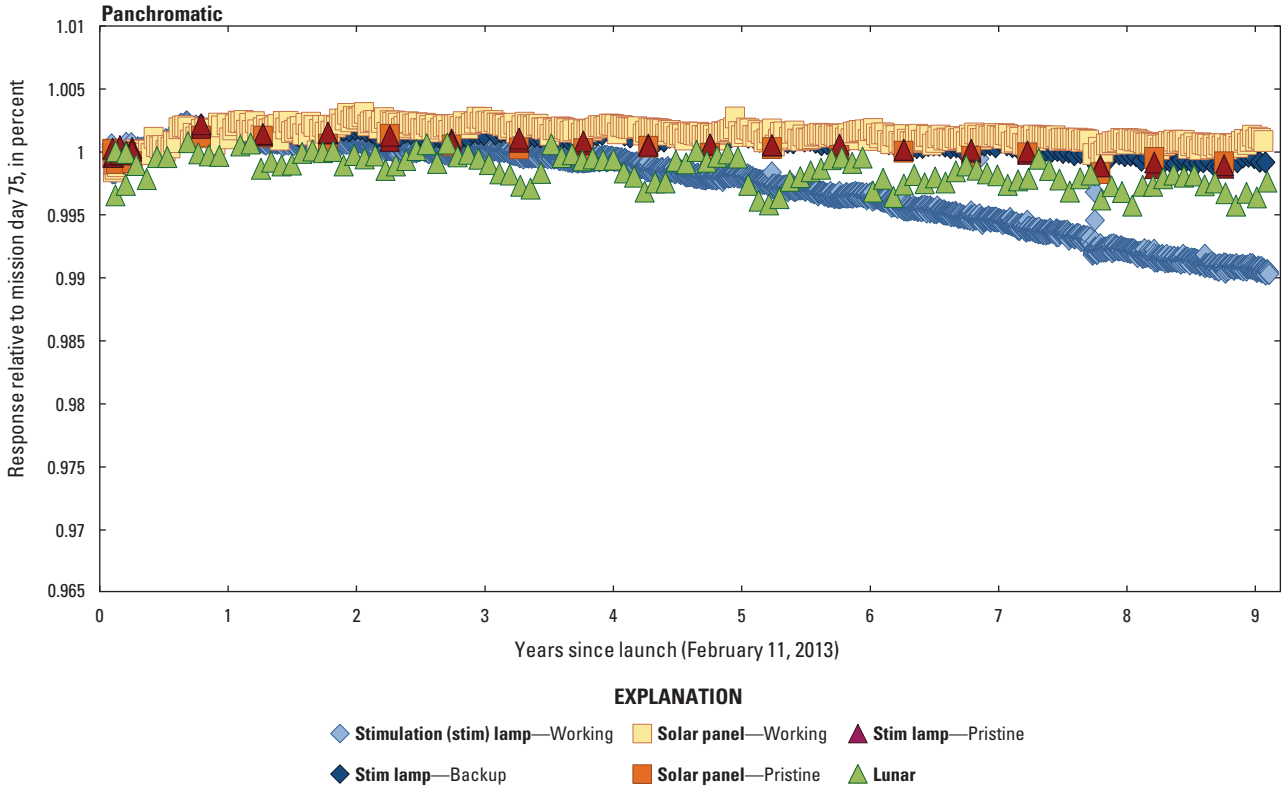

Figure 20. Landsat 8 Operational Land Imager panchromatic band lifetime radiometry stability.

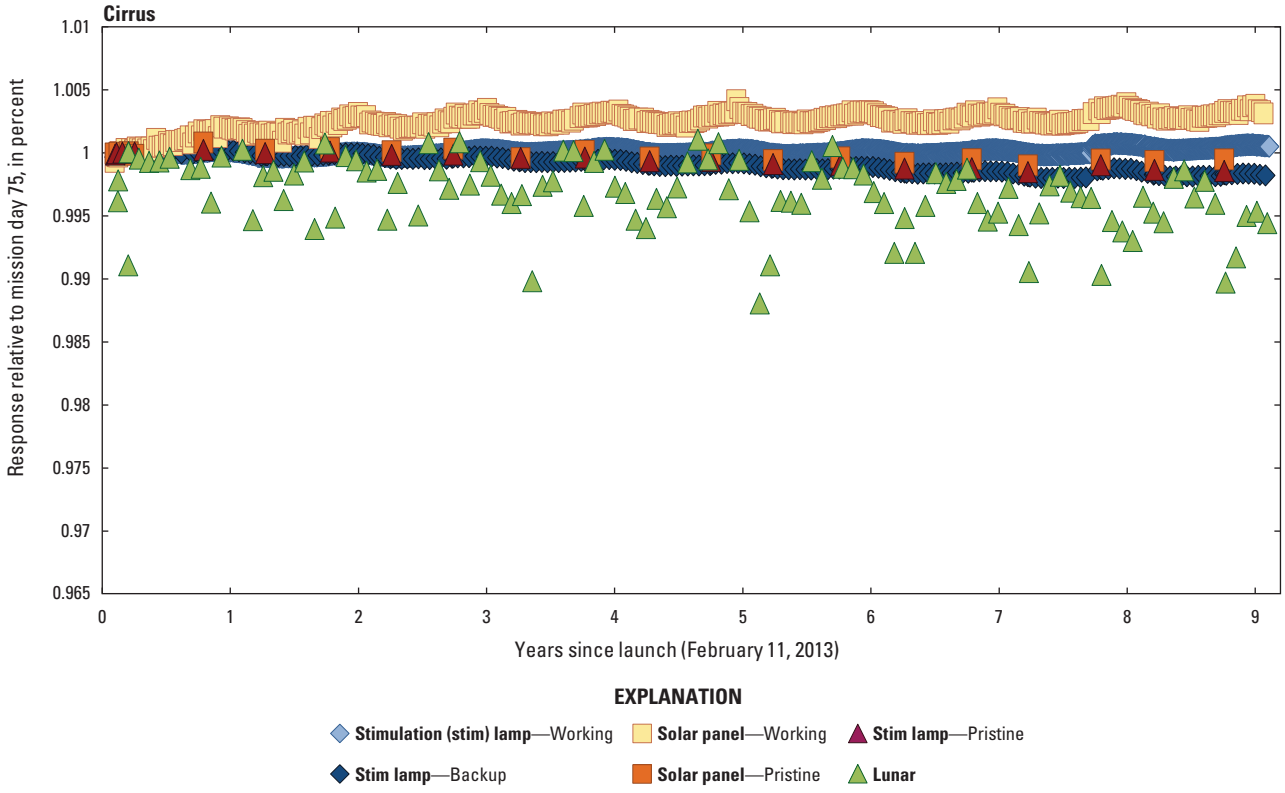

Figure 21. Landsat 8 Operational Land Imager cirrus band lifetime radiometric stability.

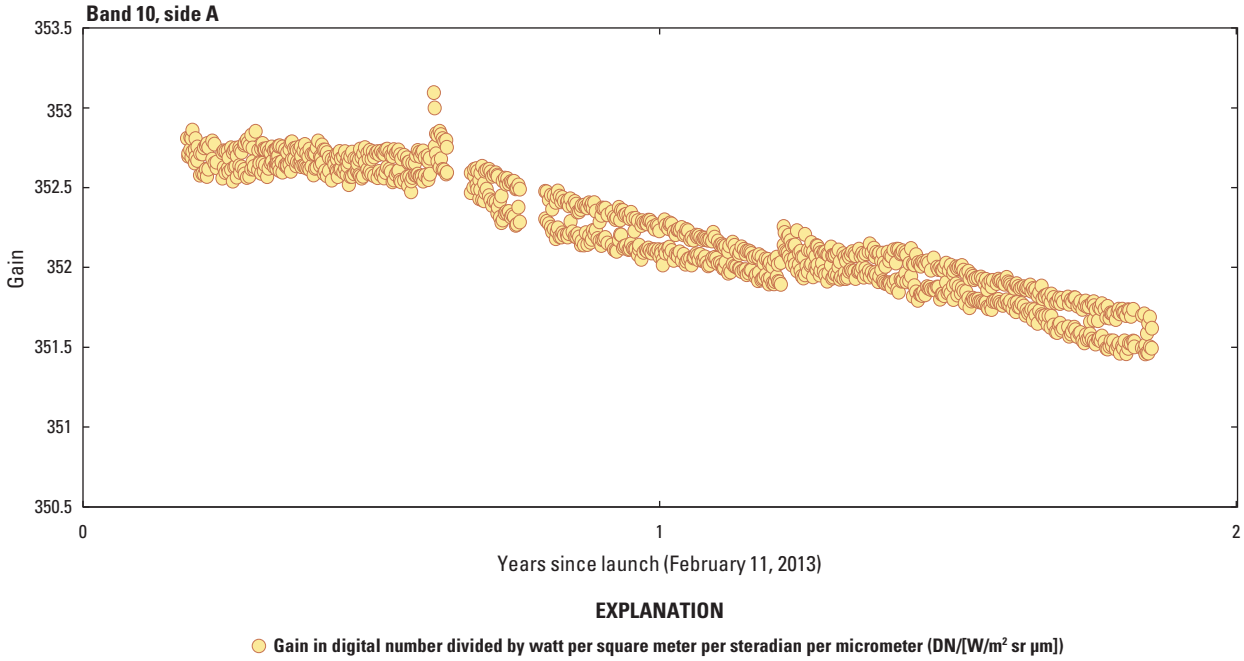

Figure 22. Landsat 8 Thermal Infrared Sensor band 10 radiometric stability (side A).

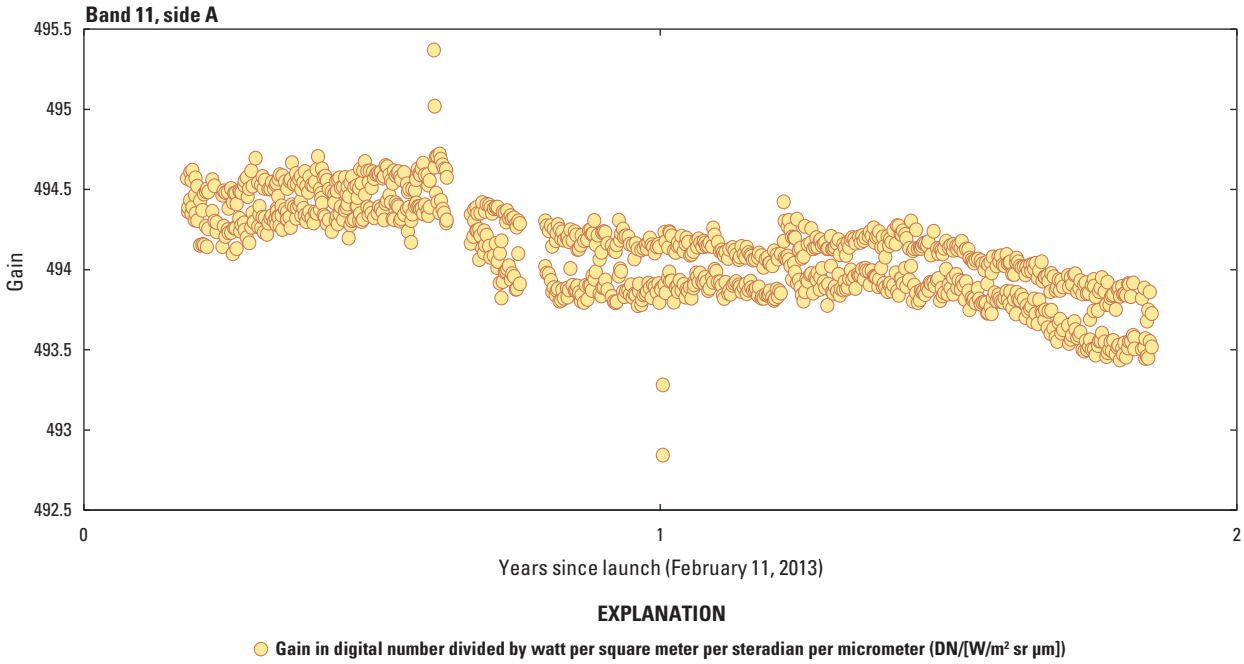

Figure 23. Landsat 8 Thermal Infrared Sensor band 11 radiometric stability (side A).

on Earth Observation Satellites, 2021) are used to monitor changes in absolute calibration, and vicarious methods are used to check absolute calibration over time (USGS, 2021d). Updates can be made to the calibration parameters used in processing the data to L1 when substantial change is detected in the calibrator trends.

Figure 26 shows the lifetime effect of OLI gain updates. A slow decay in coastal/aerosol (CA) and blue band calibration response was observed (figs. 13 and 14). The absolute radiometric calibration for the CA band has been actively modeled since April 2015, and an update to the calibration parameters was implemented for the blue band in April 2017. In April 2018, it was determined that the response to the

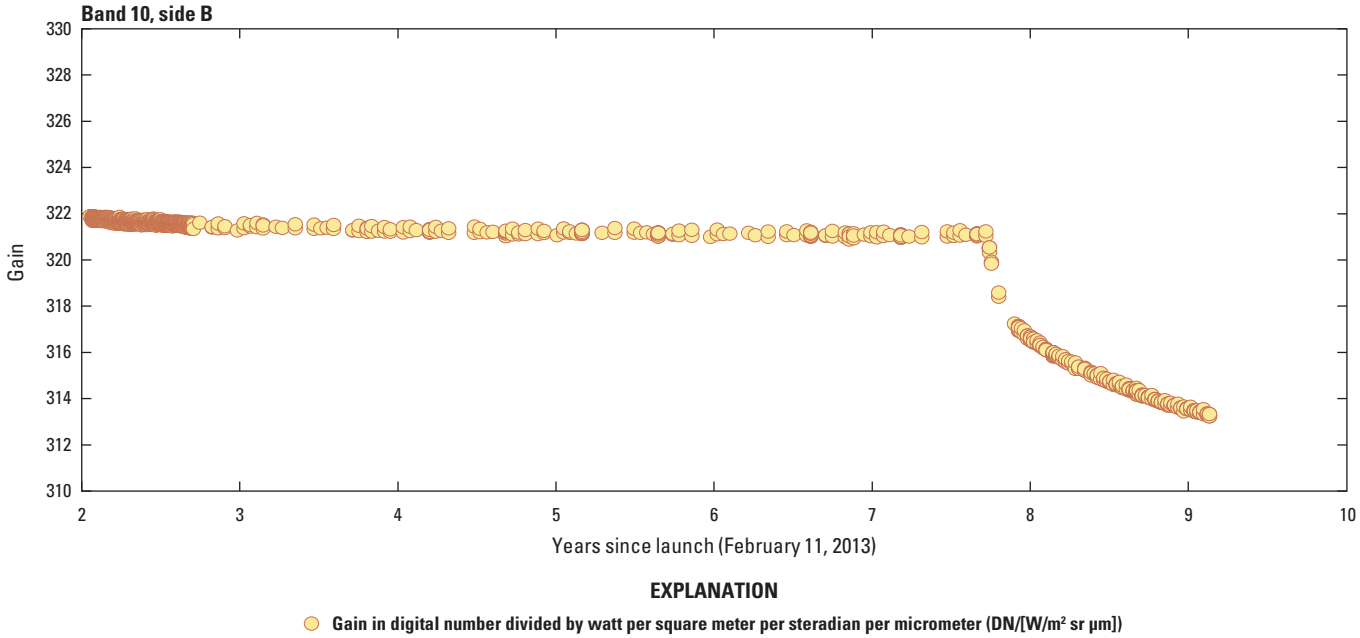

Figure 24. Landsat 8 Thermal Infrared Sensor band 10 radiometric stability (side B).

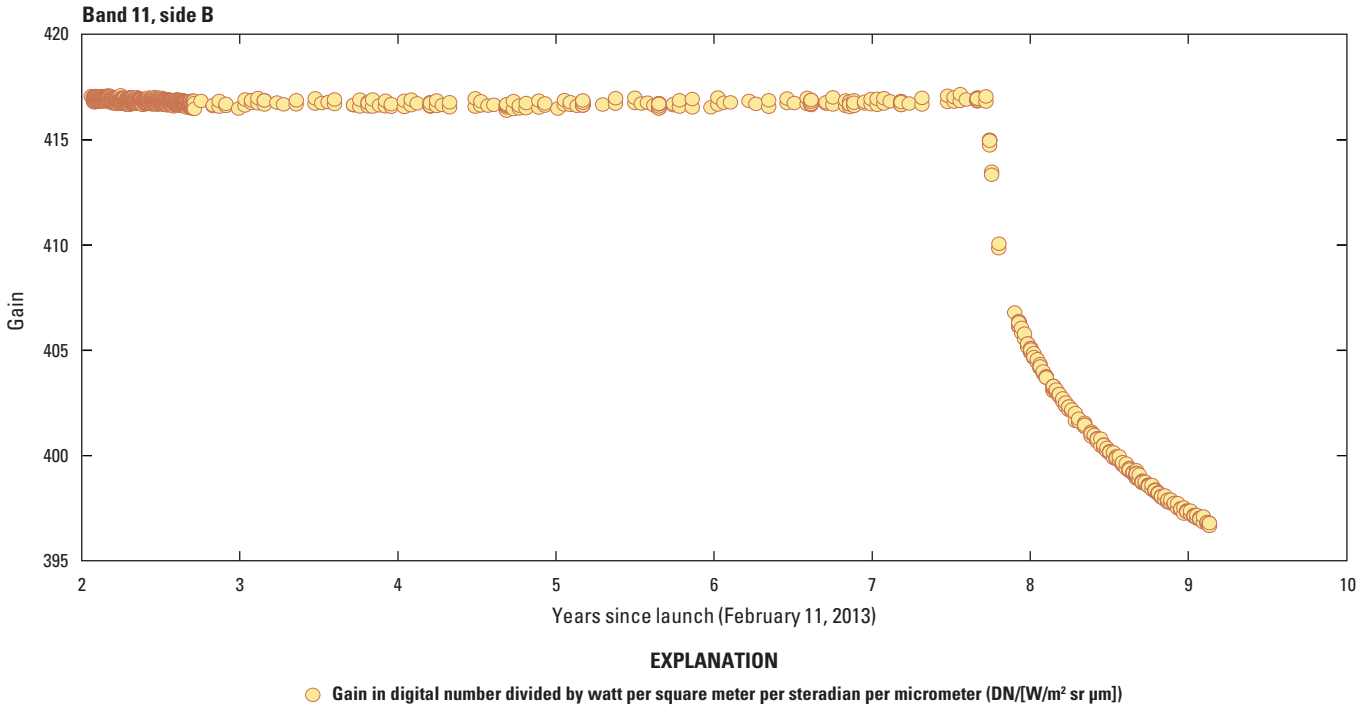

Figure 25. Landsat 8 Thermal Infrared Sensor band 11 radiometric stability (side B).

working stimulation lamp was diverging from the other calibrators, and it was removed from the model that generates the gain updates. Similarly, in October 2019, the working diffuser was removed from the gain model because of diverging trends. In both cases, the new estimates of the radiometric gain were only applied to newly acquired data. When the archive was reprocessed for Collection 2, the updated gains were applied to all data, which changed the calibrated response in the CA and blue bands by as much as 0.15 percent compared to the Collection 1 products. The safehold events in November 2020 caused small changes to the OLI response, as reflected in the figure by the small, systematic error adjustments that were

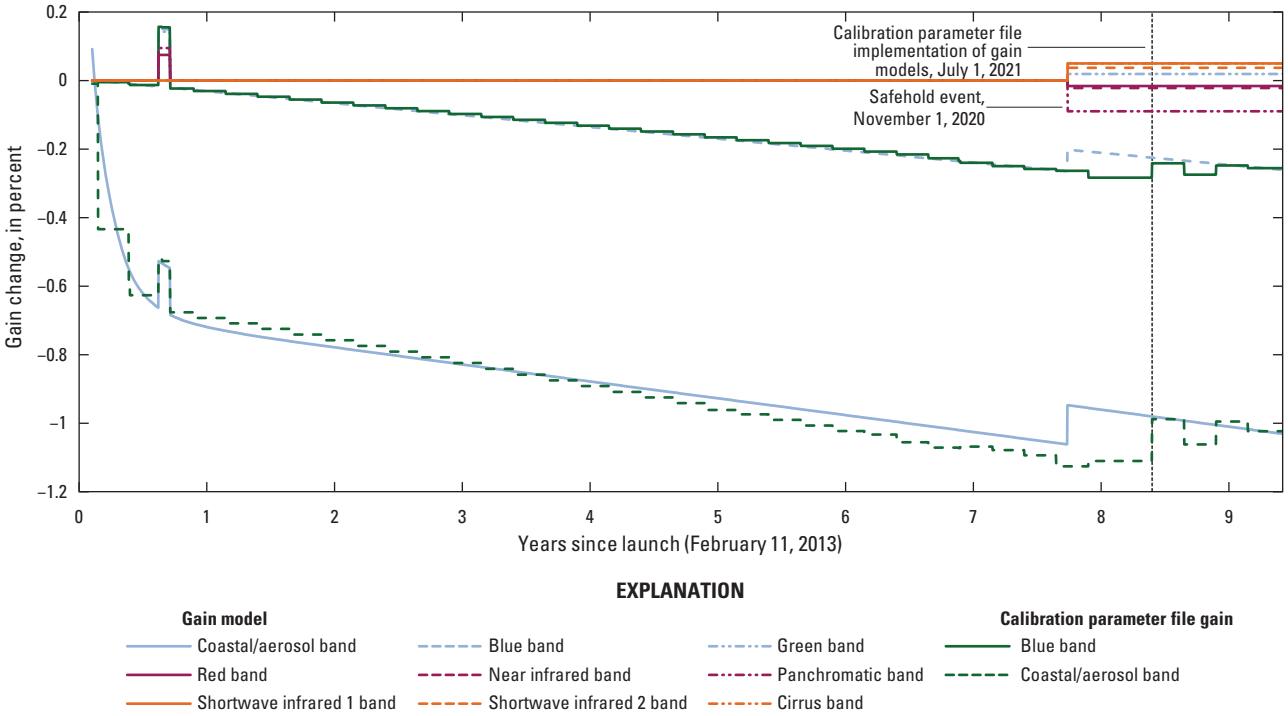

Figure 26. Landsat 8 Operational Land Imager lifetime gain trends and calibration gain updates.

made to the gain models. In July 2021, the calibration parameter file (CPF) was updated to account for up to a 0.12-percent step change in OLI responsivity caused by the November 2020 safehold events.

Figure 27 shows the effect of change in average gain for TIRS bands 10 and 11 since the safehold event on November 1, 2020. The orange line is a modeled gain trend for band 10 based on the internal calibrator data (fig. 23), and the blue line is the gain trend sampled into calibration parameters that ensure that there is no more than 0.5-percent band-average radiometric gain change over the CPF period in the L1 products. Likewise, for band 11, the magenta line is a modeled gain trend based on the internal calibrator data (fig. 25), and the yellow line is the gain trend sampled into calibration parameters. Because of the relatively sharp decrease in response shortly after the safehold events, calibration parameters were issued more frequently to ensure high quality L1 products. As the rate of degradation has slowed, updated calibration parameters are issued less frequently.

Relative Gains

Relative gains account for the differences in responsivity between detectors within a spectral band. OLI relative gains are monitored using solar diffuser acquisitions, side slither acquisitions (which entail a 90-degree yaw maneuver over an invariant site to flatten the data), and scene statistics. Quarterly updates are performed using data from the solar diffuser acquisitions from quarter 4 (October–December), 2021. Starting with the release of Collection 2, TIRS relative gain calibration updates were also performed quarterly using blackbody collects from the previous quarter. These calibration updates removed detector-to-detector striping (USGS, 2021d).

Figures 28, 29, 30, and 31 display typical per-detector change in relative gains between the previous quarter and this quarter for several bands by analyzing data from within each quarter. In each figure, the x-axis indicates the detector number, and the y-axis indicates the change in relative gain between the quarters as a ratio. These changes in responsivity are accounted for in the L1 product by updating the following quarter's CPF.

Figures 32 and 33 indicate the OLI detectors that have displayed a sudden change in responsivity of 0.5 percent or higher in the shortwave infrared (SWIR) 1 and SWIR 2 bands since launch. The x-axis indicates the date that the jump in responsivity occurred, and the y-axis signifies the detector number. These "jumpers" seem to be randomly scattered in time and location on the focal plane so do not seem to be associated with any particular instrument event or failure. These jumps are only seen in the SWIR bands (SWIR 1, SWIR 2, and cirrus); the visible and near infrared band detectors have not exhibited any jumper behavior over the whole mission.

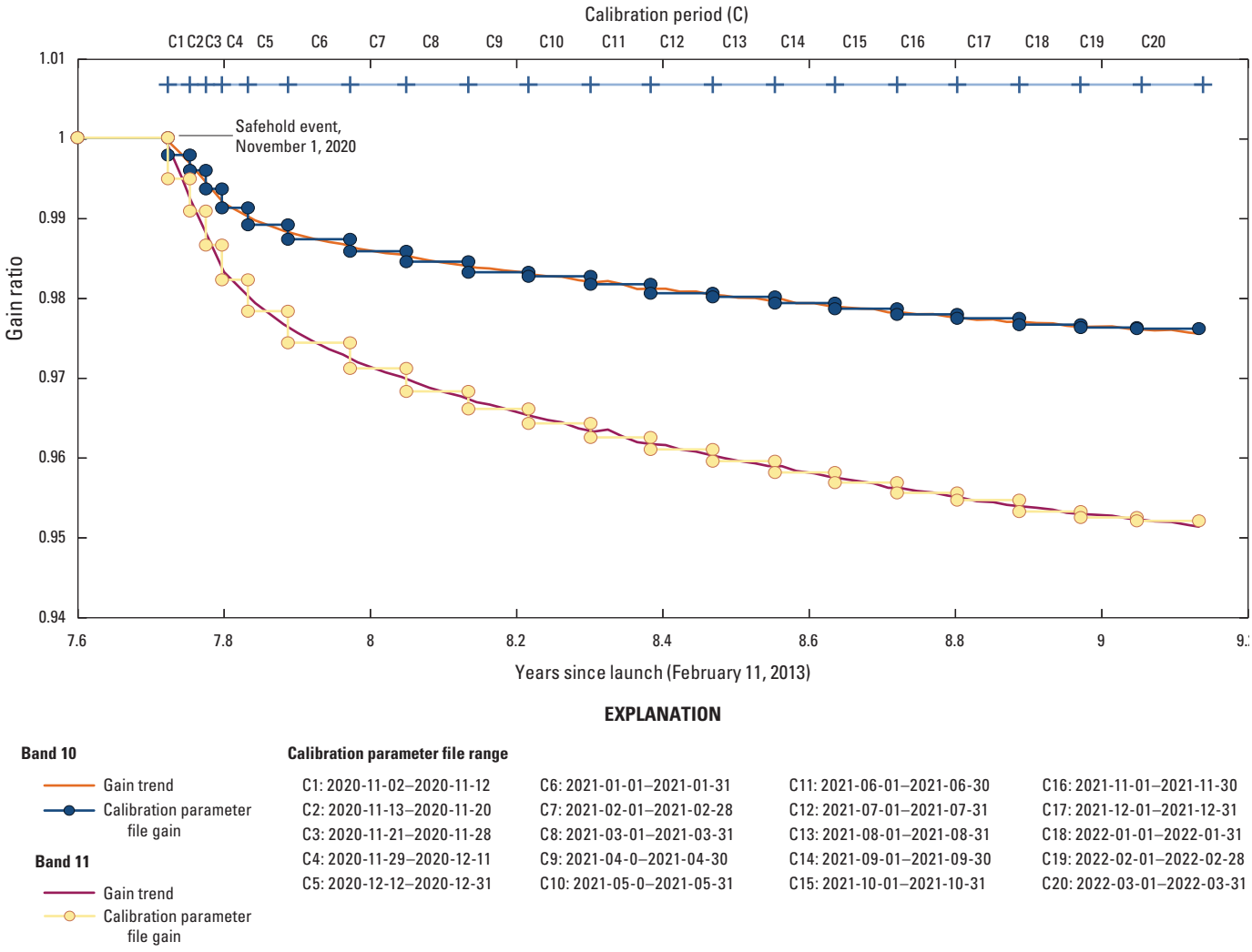

Figure 27. Landsat 8 Thermal Infrared Sensor gain degradation since the safehold event on November 1, 2020.

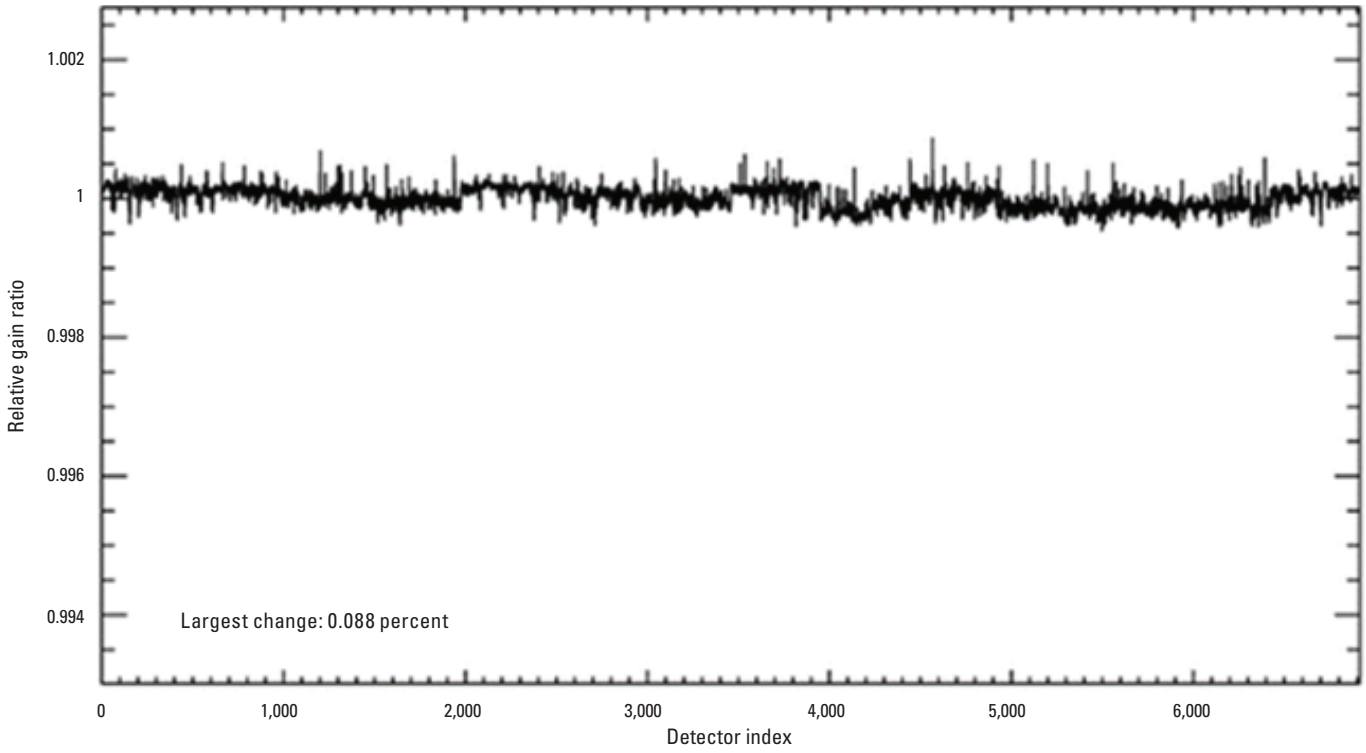

Figure 28. Landsat 8 Operational Land Imager coastal/aerosol band per-detector change in relative gains between quarter 4, 2021, and quarter 1, 2022.

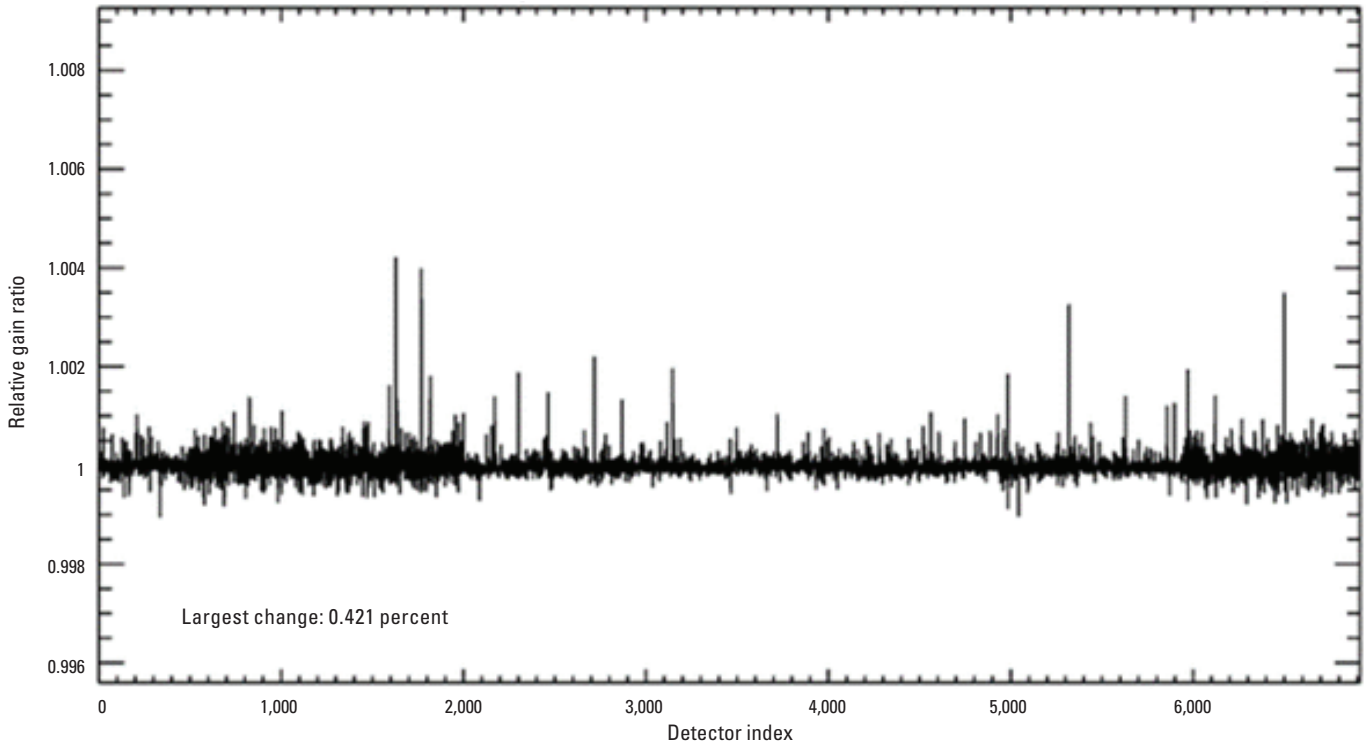

Figure 29. Landsat 8 Operational Land Imager shortwave infrared 1 band per-detector change in relative gains between quarter 4, 2021, and quarter 1, 2022.

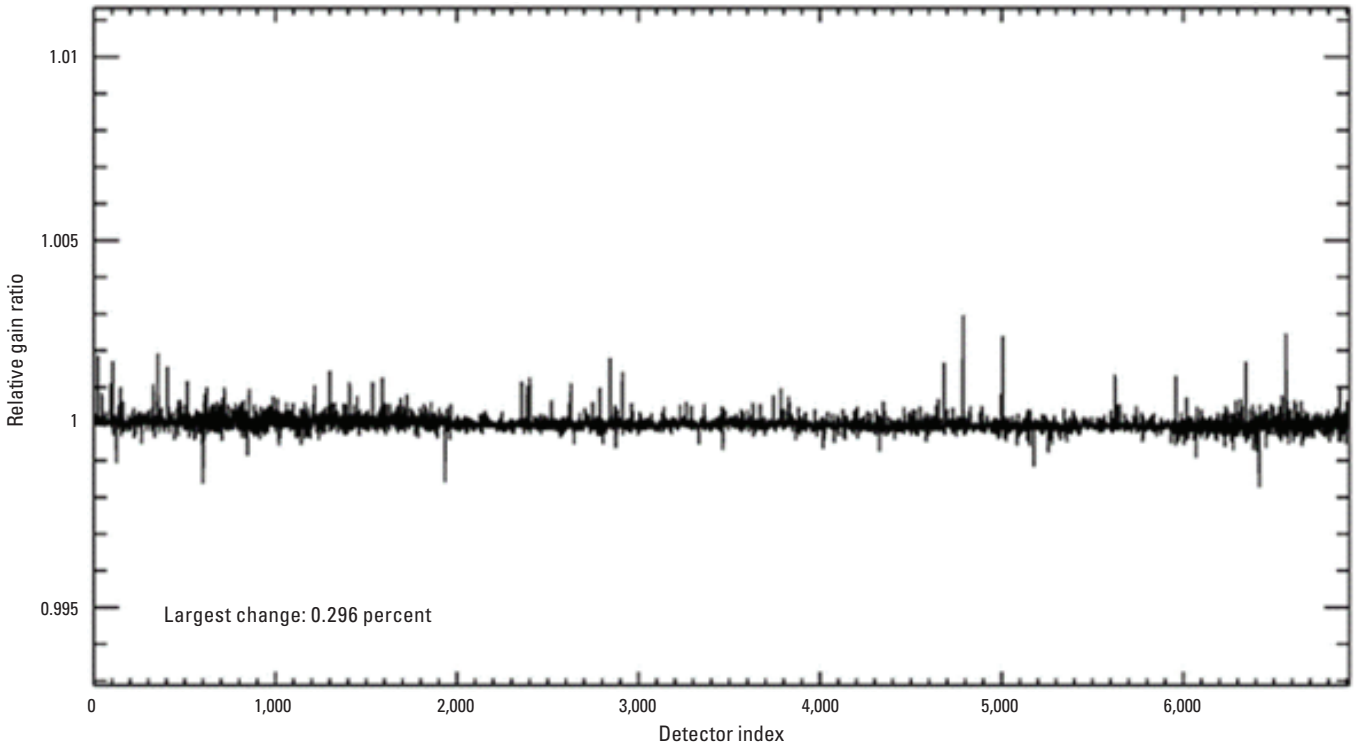

Figure 30. Landsat 8 Operational Land Imager shortwave infrared 2 per-detector change in relative gains between quarter 4, 2021, and quarter 1, 2022.

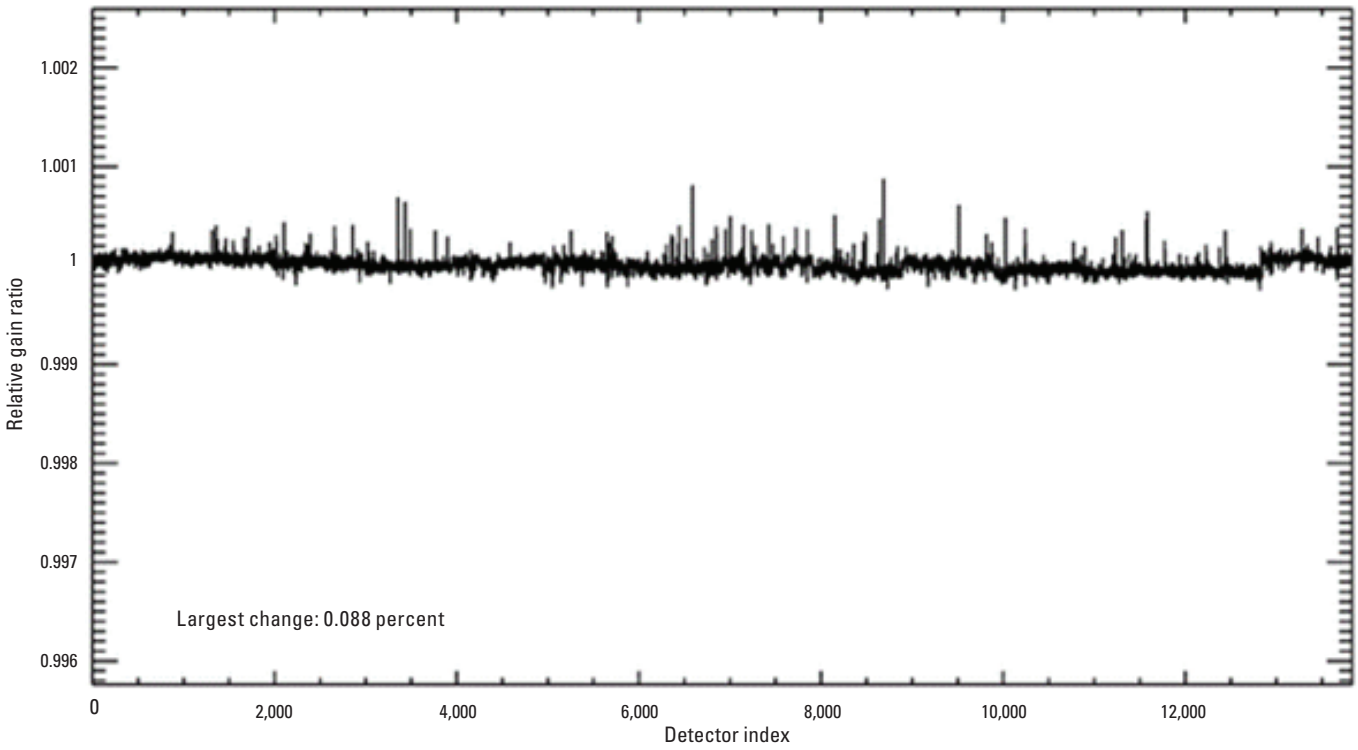

Figure 31. Landsat 8 Operational Land Imager panchromatic band per-detector change in relative gains between quarter 4, 2021, and quarter 1, 2022.

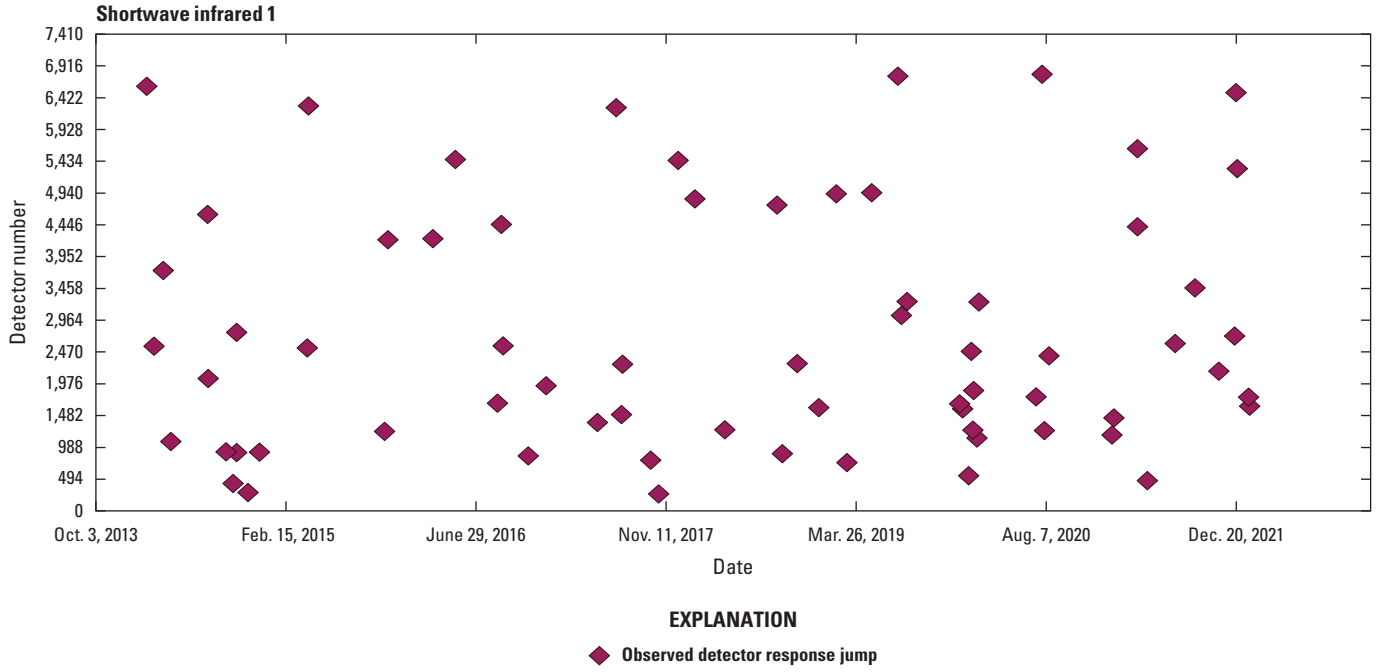

Figure 32. Landsat 8 Operational Land Imager shortwave infrared 1 lifetime jumps in detector responsivity.

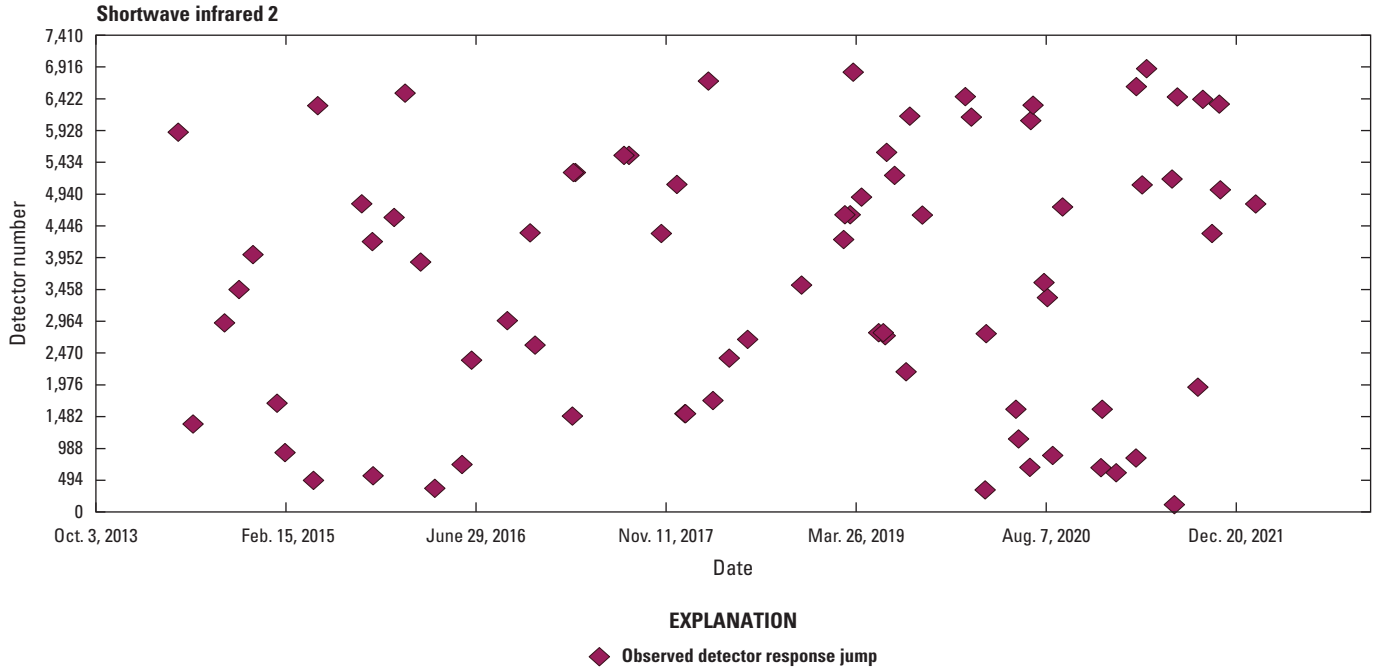

Figure 33. Landsat 8 Operational Land Imager shortwave infrared 2 lifetime jumps in detector responsivity.

Landsat 8 Geometric Performance Summary

Geometric Performance Summary

The Landsat 8 on-orbit geometric performance for the reporting quarter (quarter 1, January–March 2022) mostly meets all requirements as outlined in USGS (2019b). Geometric L1 terrain corrected product (L1T) accuracy for this quarter slightly exceeds the required value of 12 meters, likely due to the number of cloudy scenes that were included in the trending calculations. All additional geometric measurements meet the requirements. The quarterly results summary is provided in table 4.

Band Registration Accuracy

Internal band registration measures how accurately the various Landsat 8 spectral bands are geometrically aligned to each other. The assessment provides a numerical evaluation of the accuracy of the band registration within an image, using automated cross-correlation techniques between the bands to be assessed (USGS, 2021d).

OLI band registration performance has been very stable over time. Figure 34 shows quarterly band-to-band maximum registration accuracy for each band combination except for the cirrus band. Within the figure, blue bars indicate maximum registration accuracy in the line direction and green bars indicate maximum registration accuracy in the sample direction. Lifetime OLI band registration accuracy for all bands is 4.2 meters (not shown), and lifetime OLI band registration accuracy for all bands, excluding cirrus, is 3.3 meters, which is well within the instrument specification accuracy. OLI band registration accuracy for all bands during quarter 1, 2022, is 3.5 meters (not shown), and OLI band registration accuracy for all bands excluding cirrus during quarter 1, 2022, is 3.3 meters.

TIRS band registration performance has been stable throughout the instrument's lifetime, including after changes in scene select mechanism (SSM) operation beginning in December 2014. Behavior is well within specification, as shown in figure 35, and quarter 1, 2022, results are consistent with past performance. Within the figure, blue bars indicate maximum registration accuracy in the line direction, and green bars indicate maximum registration accuracy in the sample direction. Lifetime TIRS band registration accuracy is 9.1 meters, and during quarter 1, 2022, the accuracy is 8.3 meters. Since quarter 3 (July–September), 2020 (Collection 2 data), registration bias between the line and sample directions has reduced, which may be because of better SSM pointing stability, the TIRS relative gain update, or both.

Figure 36 shows lifetime TIRS to OLI band registration accuracy by quarter. Before the Collection 2 CPF update, seasonal effects are noticeable but leveled off after the release of Collection 2 in December 2020, as indicated by the closely aligned line (blue bars) and sample (green bars) accuracies. Lifetime TIRS to OLI registration accuracy (excluding the cirrus band) is 19.1 meters in the line direction and 17.5 meters in the sample direction. Quarter 1, 2022, TIRS-to-OLI registration accuracy (excluding the cirrus band) is 18.8 meters in the line direction and 17.3 meters in the sample direction.

Operational Land Imager to Thermal Infrared Sensor Alignment

OLI to TIRS alignment knowledge is critical to ensure that the L1 product accuracy requirements can be met. The alignment between OLI and TIRS instruments is periodically measured using correlation-based methods to ensure that the band-to-band alignment requirements for all Landsat 8 bands can be met (USGS, 2021d). The alignment estimates are used to update the calibration parameters in the CPFs when the observed changes are found to affect the performance requirements.

Table 4. Landsat 8 geometric performance summary, quarter 1, 2022.

[The previous quarter is quarter 4, 2021. OLI, Operational Land Imager; <, less than; LE90, linear error with 90-percent confidence; CE90, circular error with 90-percent confidence; L1T, Level 1 terrain corrected product; >, greater than; TIRS, Thermal Infrared Sensor]

Requirement	Measured value from this quarter	Measured value from previous quarter	Required value	Unit
OLI band registration accuracy (all bands)	3.5	4.8	<4.5	Meter (LE90)
OLI band registration accuracy (no cirrus)	3.3	3.2	<4.5	Meter (LE90)
Absolute geodetic accuracy	29.7	21.6	<65	Meter (CE90)
Relative geodetic accuracy	8.0	7.2	<25	Meter (CE90)
Geometric (L1T) accuracy	12.6	10.2	<12	Meter (CE90)
OLI edge slope	0.0290	0.0300	>0.027	1 per meter
TIRS band registration accuracy	8.3	8.2	<18	Meter (LE90)
TIRS-to-OLI registration accuracy	18.8	18.6	<30	Meter (LE90)

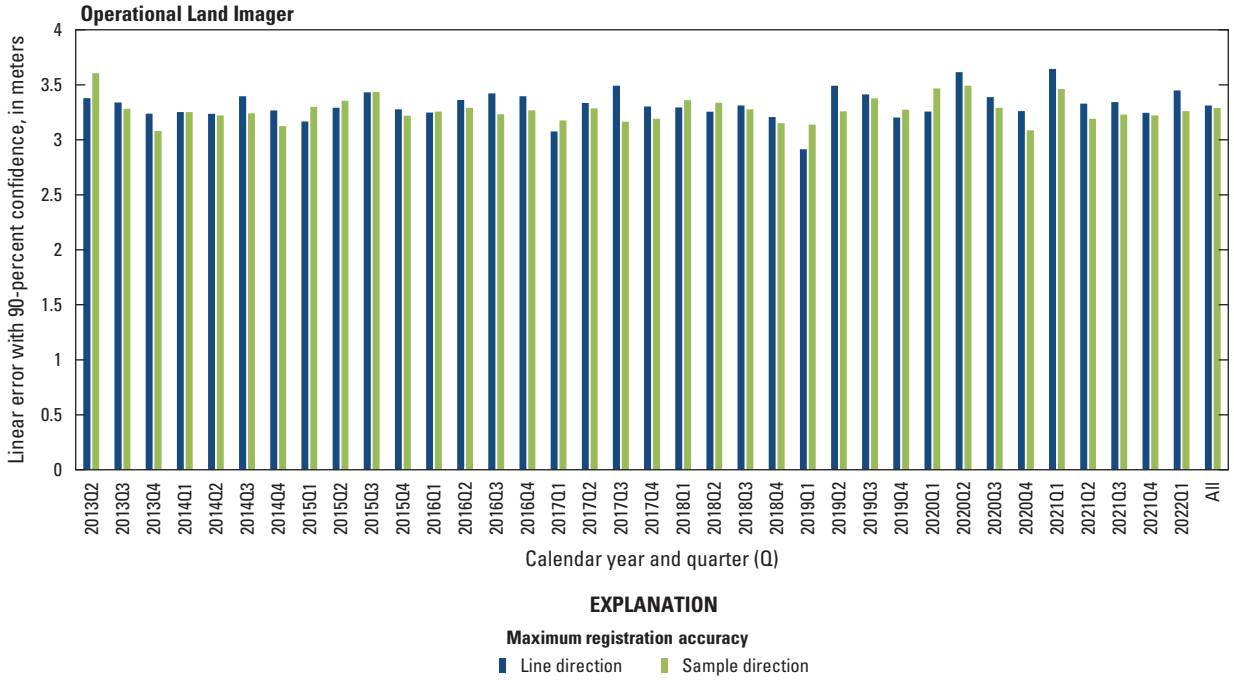

Figure 34. Operational Land Imager lifetime band (excluding cirrus) registration accuracy by quarter.

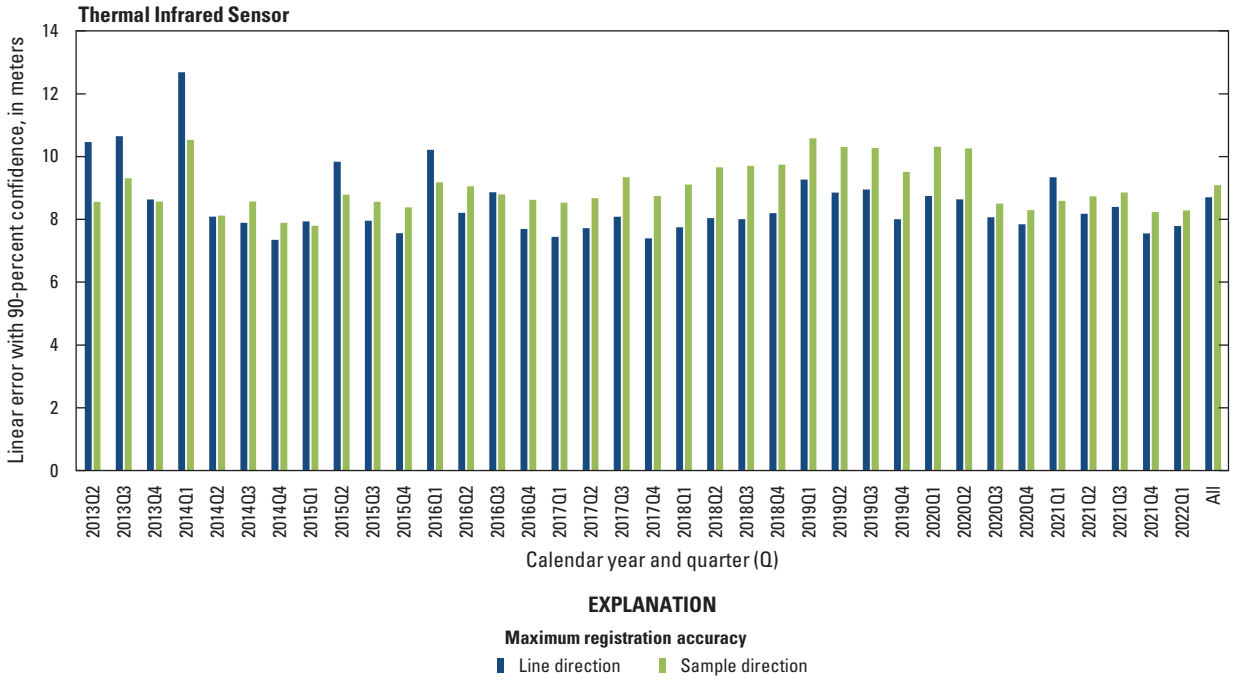

Figure 35. Landsat 8 Thermal Infrared Sensor lifetime band registration accuracy by quarter.

Figure 37 shows TIRS to OLI pitch alignment measurements over instrument lifetimes. The November 2020 safehold events did substantially affect pitch alignment, but the Cal/Val Team continues to monitor this. Recently (in quarter 4, 2021), a small change in the TIRS to OLI pitch alignment was observed, which is similar to the seasonal trend observed in previous years. However, the magnitude of this trend was not the same as before, so it was unclear whether this new trend would continue or not. The trend continued in quarter 1, so a CPF update will be issued in quarter 2 (April–June), 2022, for

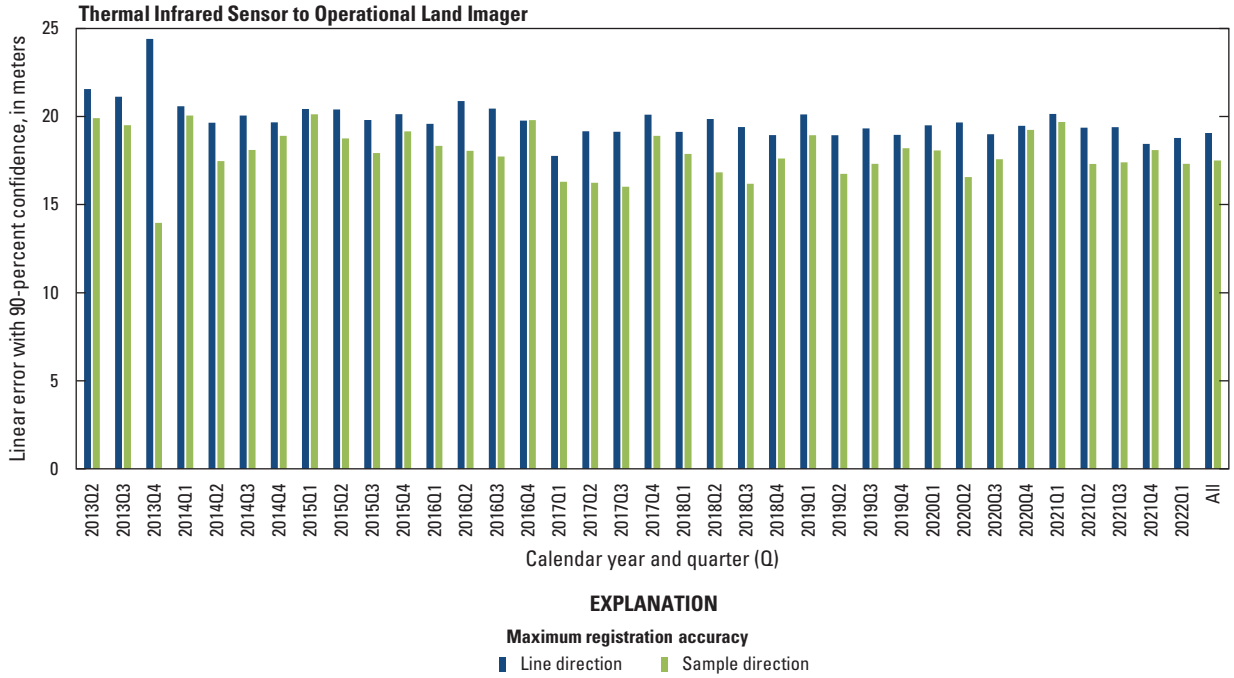

Figure 36. Landsat 8 Thermal Infrared Sensor to Operational Land Imager lifetime band (excluding cirrus) registration accuracy by quarter.

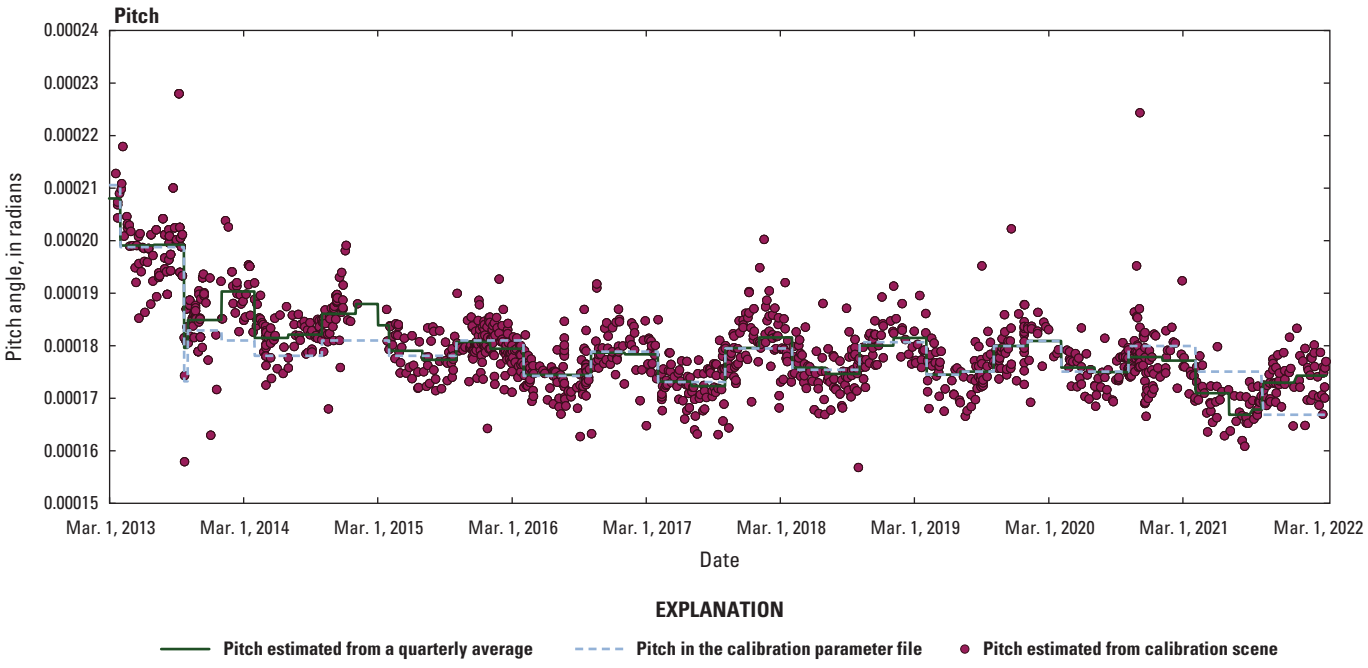

Figure 37. Landsat 8 Thermal Infrared Sensor to Operational Land Imager lifetime pitch alignment.

residual corrections to the alignment parameters. Figure 38 shows the lifetime TIRS to OLI roll alignment, and figure 39 shows the lifetime TIRS to OLI yaw alignment. Each magenta symbol on these figures represents one calibration scene, the green solid lines indicate quarterly alignment averages, and the blue dashed lines indicate applied Collection 2 CPF correction values.

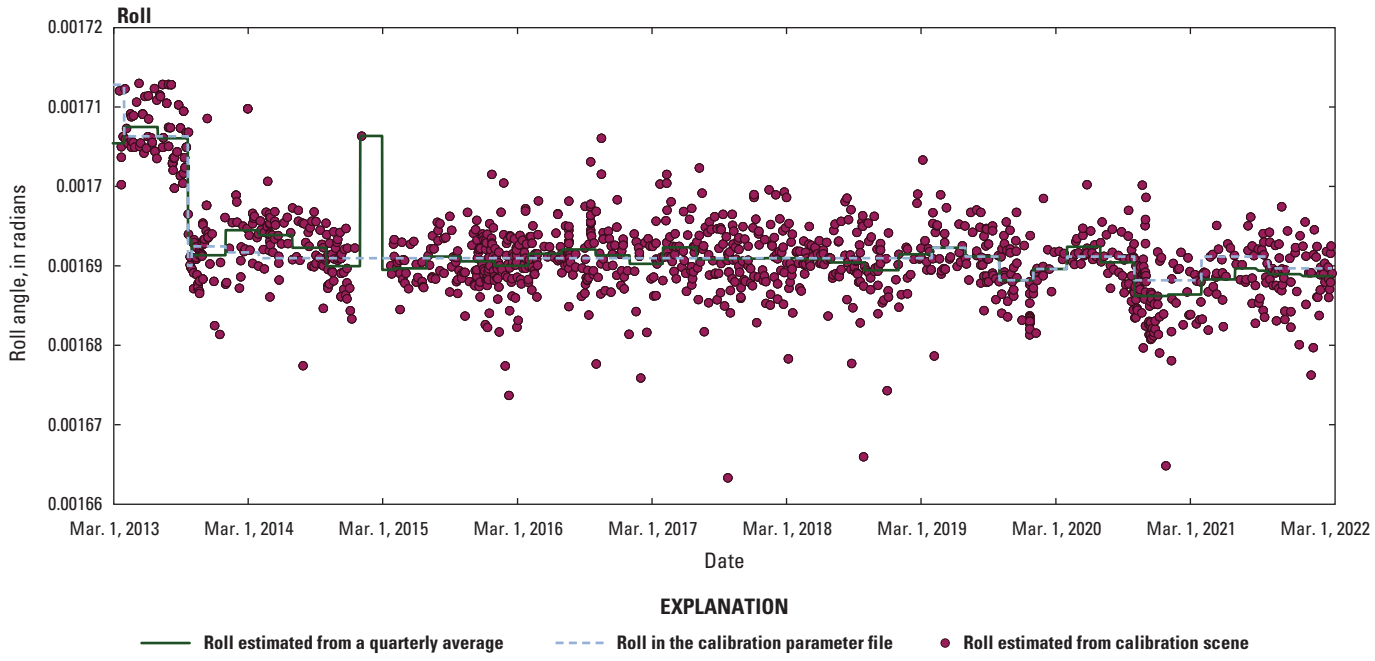

Figure 38. Landsat 8 Thermal Infrared Sensor to Operational Land Imager lifetime roll alignment.

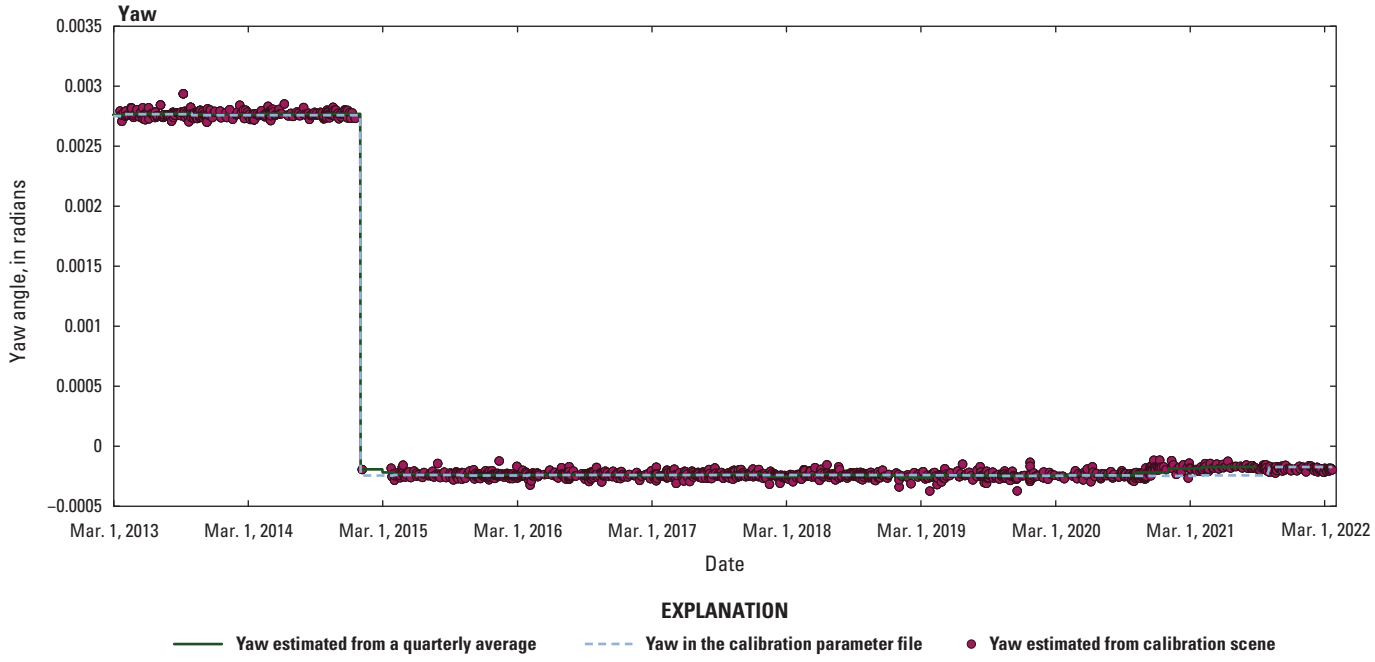

Figure 39. Landsat 8 Thermal Infrared Sensor to Operational Land Imager lifetime yaw alignment.

Geometric Accuracy

Landsat 8 geometric assessment evaluates the absolute positional accuracy of the image products with respect to a ground (geometric) reference. The geometric accuracy assessment estimates the geometric error between the L1TP products and GCPs using automated cross-correlation techniques (USGS, 2021d).

Based on analysis results, relative accuracy of the Collection 2 GCPs is comparable to the digital orthophoto quadrangle (DOQ) supersites, which are sites created from a mosaic of highly accurate high-resolution terrain-corrected

aerial data. Comparatively, relative accuracy of the Collection 2 GCPs is substantially better than the internal consistency of the Collection 1 GCPs. Overall, cloud contaminated scene-based results are the primary contributor to poor geometric accuracy from L1TP products. Figure 40 provides lifetime quarterly geometric accuracy at a circular error with 90-percent confidence (CE90). Blue bars indicate the geometric accuracy estimated over supersite path/rows (calibration site) using DOQ GCPs, yellow bars indicate geometric accuracy estimated over supersite path/rows (calibration site) using Collection 2 GCPs, and green bars indicate geometric accuracy estimated over all L1TP scenes processed in Collection 2 using Collection 2 GCPs. All results are consistently within the accuracy specification.

Lifetime and quarter 1, 2022, geometric accuracies for L1TP products are 3.8 and 4.4 meters when compared against DOQ controls over supersite path/rows, 5.4 and 6.8 meters when compared against Collection 2 GCPs over supersite path/rows, and 9.7 and 12.6 meters when analyzing all the L1TP scenes processed in Collection 2, respectively. Note that seasonal effect is a factor in accuracy results.

Geodetic Accuracy

The purpose of the geodetic accuracy assessment is to ensure that the Landsat 8 L0Rp data can be successfully processed into L1 systematic products that meet the system requirement of 65 meters at a CE90 horizontal accuracy. To measure the accuracy, calibration scenes are automatically correlated with data from the panchromatic band to measure the discrepancy between the known ground location and the position predicted by the OLI geometric model (USGS, 2021d).

Based on analysis results, absolute accuracy of the Collection 2 GCPs is comparable to the DOQ supersites and is substantially better compared to the Collection 1 GCPs (Rengarajan and others, 2020). Figure 41 provides lifetime quarterly geodetic accuracy (CE90). Blue bars indicate the accuracy estimated using DOQ supersite path/rows (calibration site), and green bars indicate accuracy estimated from all L1TP scenes processed in Collection 2 using Collection 2 GCPs. As in the case with the geometric accuracy, a wide variety of scene types (cloud contaminated, islands, desert, snow-covered, ice sheets, and so on) are the primary contributor to the poor geodetic accuracy for Collection 2 GCP-based results.

Although quarters 1, 2, and 3, 2021, showed a slight increase in the geodetic accuracy offset, the lifetime results have been consistently well within the accuracy specification. The recent increase in the geodetic accuracy is because of a systematic bias in the along-track direction observed since the November 2020 safehold events. The bias is now steady and an update to the sensor alignment parameters in the CPF was released in quarter 4, 2021, resulting in a decrease in the observed geodetic offsets. Lifetime and quarter 1, 2022, geodetic accuracies for systematic products are 16.7 and 19.3 meters when compared using DOQ GCPs over supersites, and 25.3 and 29.7 meters when compared using Collection 2 GCPs over all the scenes processed in Collection 2, respectively.

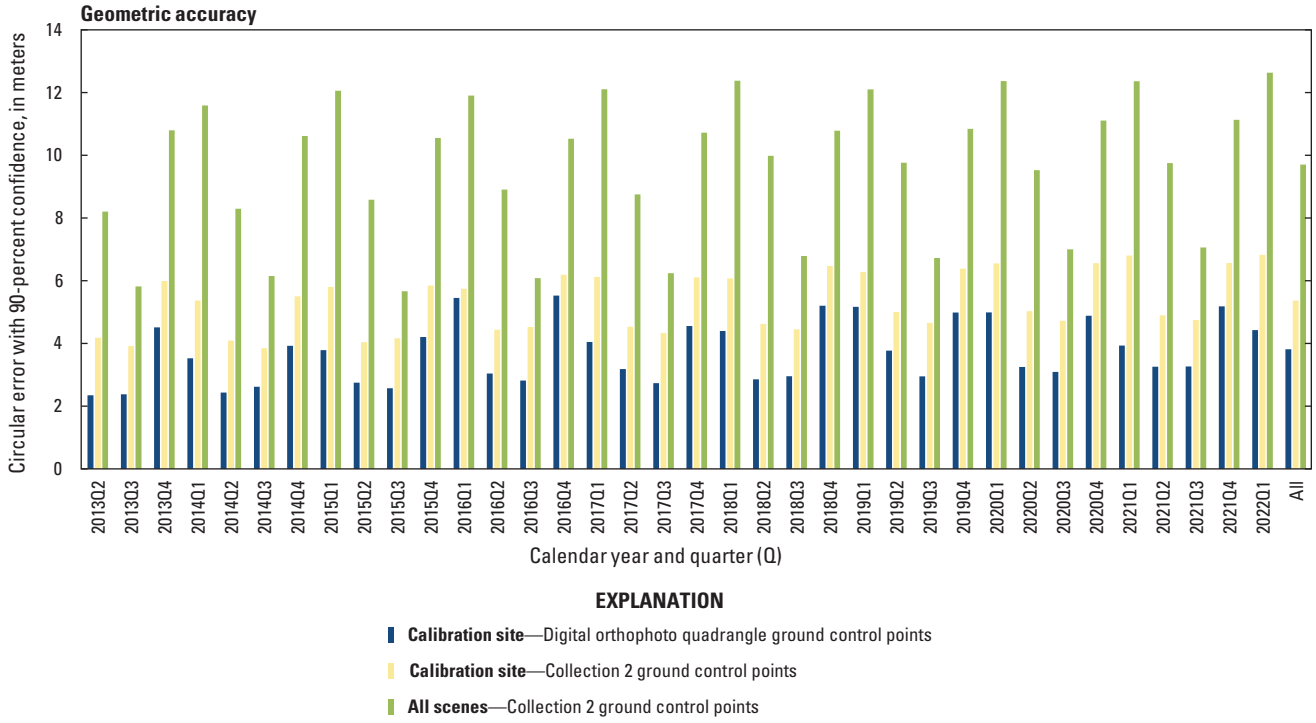

Figure 40. Landsat 8 lifetime geometric accuracy by quarter.

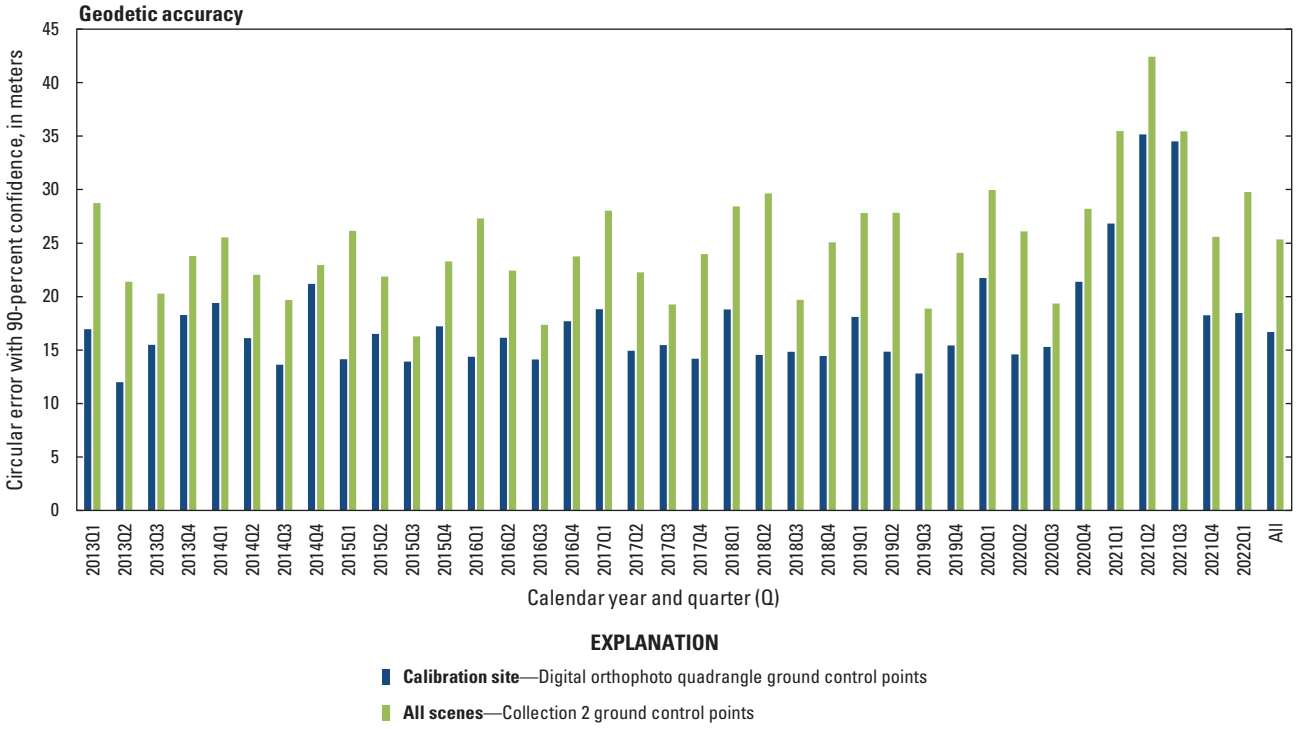

Figure 41. Landsat 8 lifetime geodetic accuracy by quarter.

Landsat 8 to Sentinel-2 Registration Accuracy

The USGS Landsat Collection 2 release included an update to the Landsat ground reference dataset by harmonizing with the Sentinel-2 Global Reference Image (GRI) dataset. The objective of using the GRI dataset in Landsat ground reference was to improve the absolute and relative accuracies of the Landsat products across all missions, as well as to improve the coregistration between Landsat and Sentinel-2 terrain-corrected products. The Cal/Val Team plans to continue to assess the coregistration error between the two sensors over a select number of sites that are globally distributed.

The European Space Agency began using GRI as reference in their Sentinel-2 L1C processing in March/April 2021, but global coverage (excluding Antarctica and small islands) was limited to scenes over Europe and Africa until August 2021. Sentinel-2 L1C products generated before GRI availability are planned to be reprocessed with GRI as a ground reference at a future date. Figure 42 shows the observed coregistration error between Landsat 8 L1TP products and Sentinel-2 L1C products without the use of GRI (as indicated with the magenta dots), as well as coregistration errors with Sentinel-2 L1C products where GRI was used (as indicated with the yellow dots). Coregistration errors without the use of GRI are expected to be less than 15 meters; coregistration errors with GRI are expected to be less than 8 meters. For reference, observed coregistration errors between Landsat 8 L1TP products are also included in the figure as indicated with the orange dots. With recent global availability of Sentinel-2 L1C products using GRI as the geospatial reference, the number of characterized sites will be expanded to a couple of tiles from each continent while also using the growing temporal inventory.

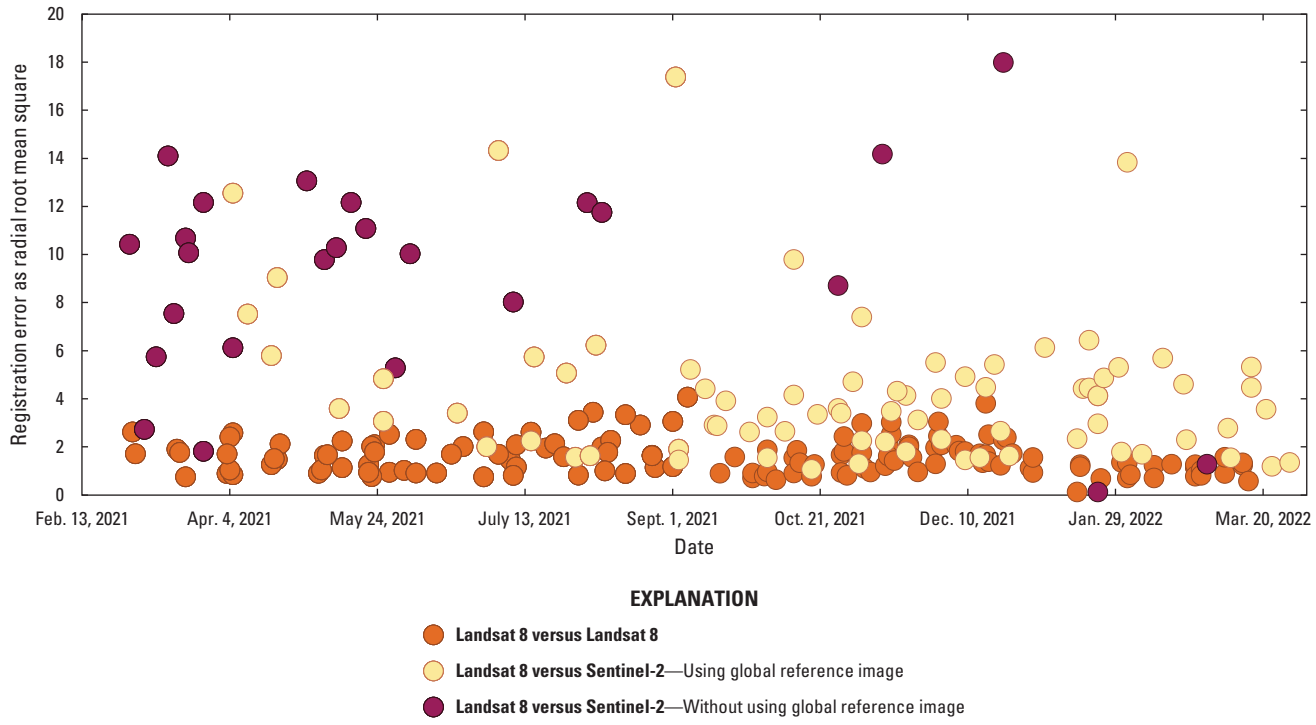

Figure 42. Landsat 8 coregistration error between Level 1 terrain corrected product and Sentinel-2 Level 1 orthorectified product since quarter 1, 2021.

Landsat 7 Radiometric Performance Summary

Onboard Calibrator Trends

The Enhanced Thematic Mapper Plus (ETM+) has three onboard calibration devices: the Internal Calibrator, the Partial Aperture Solar Calibrator, and the Full Aperture Solar Calibrator. These calibration devices have been used to monitor radiometric stability since launch (April 15, 1999; Markham and others, 1994; Barsi and others, 2016; USGS, 2019a).

The responsivity of the ETM+ as determined from the on-board calibrators is shown in figure 43 for the blue band and figure 44 for the SWIR 1 band. The three calibrators all indicate degradation over time, although at varying rates that changed at different times. The degradation shown here is thought to be primarily within the calibrators and not because of the ETM+ detectors or electronics (Markham and others, 2012).

Coherent Noise

Coherent noise in the ETM+ has been monitored since launch using a Fast Fourier transform on dark nighttime data (Barsi and others, 2016). Figure 45 displays the Landsat 7 lifetime coherent noise results for specific band and detector combinations at designated frequencies. Magnitudes of most coherent noise components remain very low, but a positive trend in coherent noise power of SWIR 1 (band 5) detector 12 (orange circles) has been observed. In this SWIR 1 detector 12 case, noise power decreases with instrument on-time along an interval, so scenes acquired earlier in an interval are subject

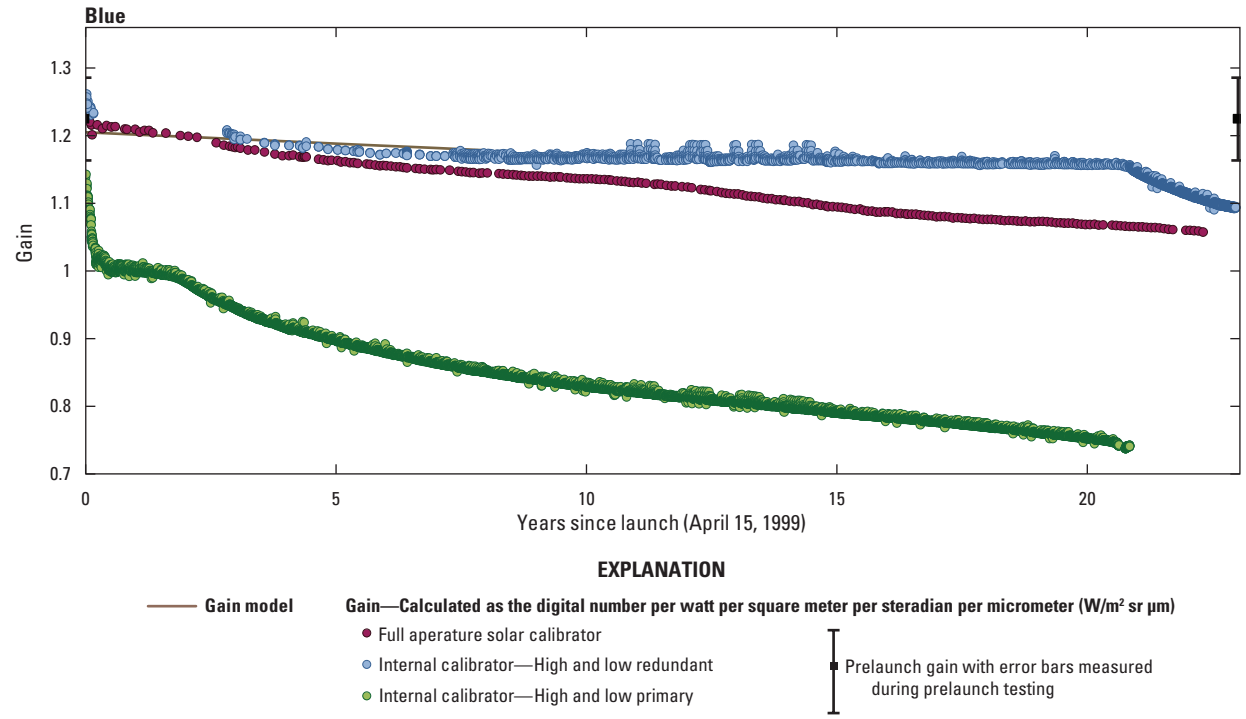

Figure 43. Landsat 7 Enhanced Thematic Mapper Plus blue band lifetime gains.

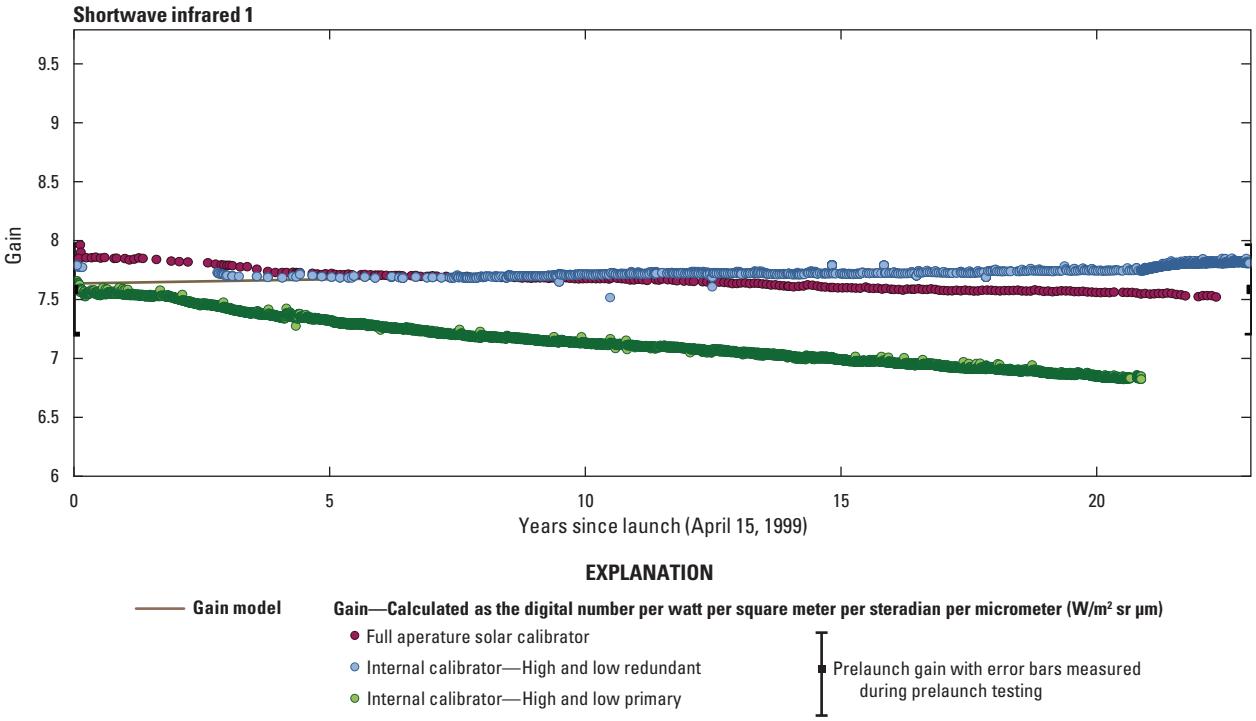

Figure 44. Landsat 7 Enhanced Thematic Mapper Plus shortwave infrared 1 band lifetime gains.

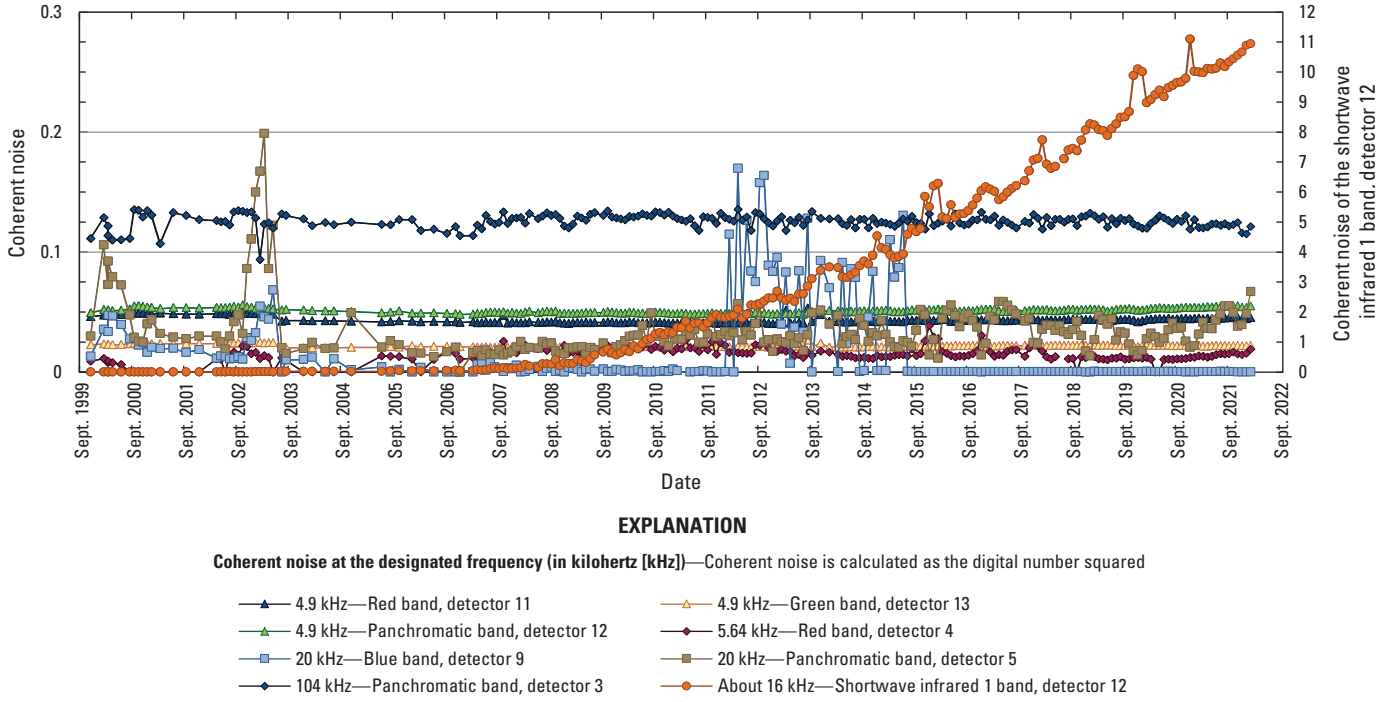

Figure 45. Landsat 7 Enhanced Thematic Mapper Plus lifetime coherent noise.

to stronger coherent noise features. In 2010, only the first few scenes acquired in an interval were affected by the coherent noise, but by 2015, the noise was strong enough that it was still present as much as 15 minutes later (fig. 45).

Pseudo-Invariant Calibration Sites Trending

PICS are also used to monitor the ETM+ radiometric stability. Several of the PICS regions (Committee on Earth Observation Satellites, 2021) defined by Centre National D'Etudes Spatiales (CNES) were used to develop a new gain model for ETM+, which was applied starting in 2013 (USGS, 2021c). The Cal/Val Team uses multiple PICS for monitoring radiometric changes because of the temporal stability of those sites. PICS trending calculates basic statistics from geographic regions of interest (ROIs) extracted from geometrically corrected Landsat products. The primary purpose for trending is to repeatedly characterize PICS, save results to the database, and thus enable an automatic monitoring of ETM+ temporal stability.

Figure 46 shows the lifetime top of atmosphere reflectance values observed over the Libya 4 PICS site (lat 28.55° N., long 23.39° E.) using the CNES ROI. The long-term temporal trends show seasonal effects, which are more substantial in the higher wavelength SWIR bands.

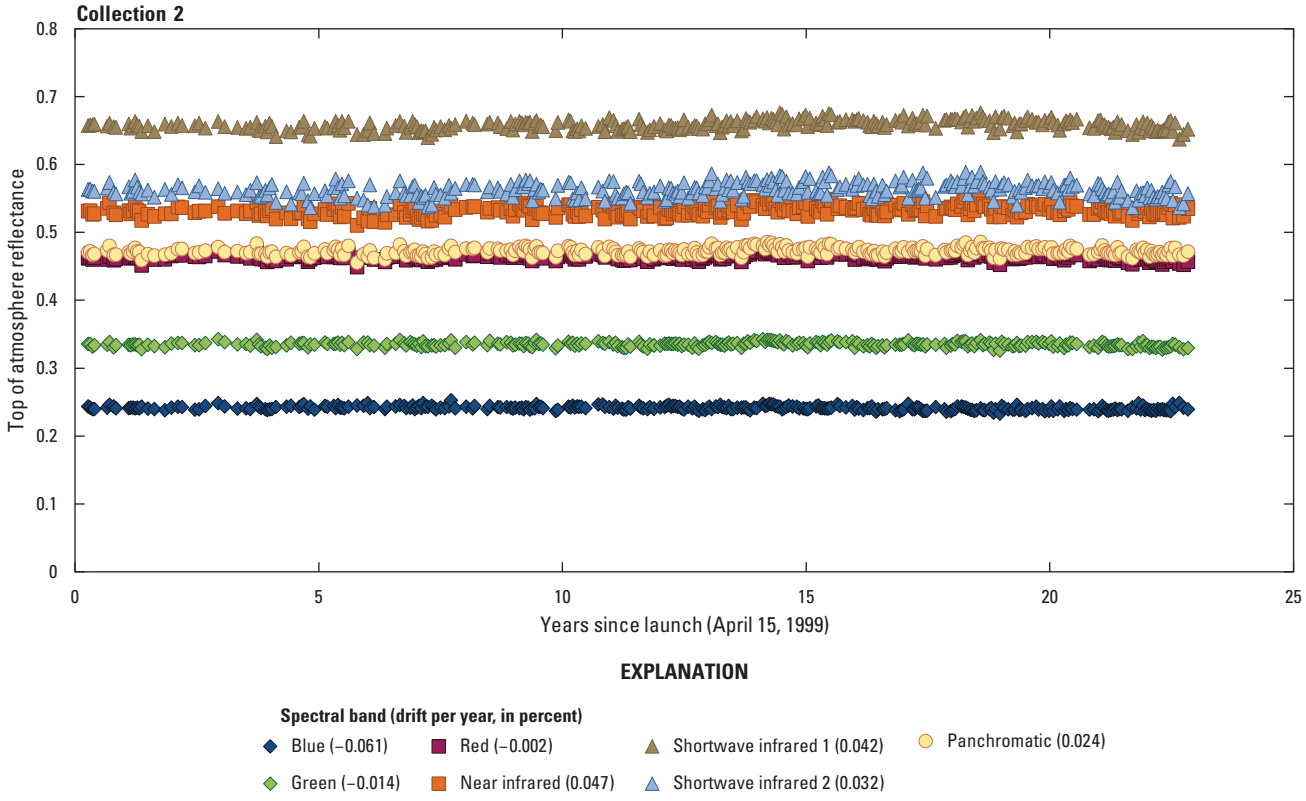

Figure 46. Libya 4 pseudo-invariant calibration site top of atmosphere reflectance trending normalizing/correcting seasonality effects, Collection 2.

After removal of the seasonal effect, there is a slight indication of deviation from current trends; the deviation is in the negative direction for the blue and green bands and in the positive direction for the near infrared, SWIR, and panchromatic bands.

Landsat 7 Geometric Performance Summary

Geometric Performance Summary

The Landsat 7 on-orbit geometric performance for this quarter (quarter 1, January–March 2022) meets all requirements as outlined in USGS (2019a). The quarterly results summary is provided in table 5.

Table 5. Landsat 7 geometric performance summary, quarter 1, 2022.

[The previous quarter is quarter 4, 2021. ETM+, Enhanced Thematic Mapper Plus; <, less than; σ, sigma; L1T, Level 1 terrain corrected product]

Requirement	Measured value from this quarter	Measured value from previous quarter	Required value	Unit
ETM+ band registration accuracy (bands 1–5, 7)	1.7	1.8	<5.1	Meter (1σ)
ETM+ band registration accuracy (thermal [band 6])	4.9	5.9	<10.2	Meter (1σ)
Absolute geodetic accuracy	107.3	100.3	<250	Meter (1σ)
Relative geodetic accuracy	12.4	10.8	<25	Meter (1σ)
Geometric (L1T) accuracy	6.3	5.6	<12	Meter (1σ)

Geodetic Accuracy

The purpose of the geodetic accuracy assessment is to ensure that the Landsat 7 L0Rp data can be successfully processed into L1 systematic products that meet the system requirement of 250-meter (1σ) accuracy, excluding terrain effects and without the use of GCPs. Geodetic accuracy is monitored using calibration supersites containing GCPs derived from the DOQ aerial photography (U.S. supersites) and Satellite Pour l'Observation de la Terre (SPOT) satellite imagery (Australian supersites).

Figure 47 displays the lifetime quarterly mean offsets for Landsat 7. Within the figure, blue bars indicate the across-track accuracy, and the green bars indicate the along-track accuracy. As of quarter 1 (January–March), 2022, this across-track offset has exceeded 80 meters.

Figure 48 displays the lifetime quarterly geodetic accuracy for Landsat 7. The figure shows the expected geodetic accuracy of a systematic product. Magenta bars indicate the across-track root mean square error (RMSE), and blue bars indicate the along-track RMSE.

Band Registration Accuracy

Internal band registration measures how accurately the various Landsat 7 spectral bands are aligned to each other. The assessment provides a numerical evaluation of the accuracy of the band registration within an image using automated cross-correlation techniques between the bands to be assessed (USGS, 2021d).

Figure 49 shows the per-band average RMSE since launch. Blue bars indicate band registration accuracy in the line direction, and green bars indicate band registration accuracy in the sample direction. This figure also shows the specification offsets, which each band easily outperforms.

Orbital Drift from Worldwide Reference System–2

Landsat 7 is nearing the end of its fuel supply. To conserve fuel, satellite inclination maneuvers have been eliminated, causing the satellite to slowly drift off of the nominal WRS–2 orbit. The Cal/Val Team continues to monitor Northern and Southern Hemisphere sites to quantify the amount of WRS–2 displacement. Stakeholders use this information to determine the useability of the data.

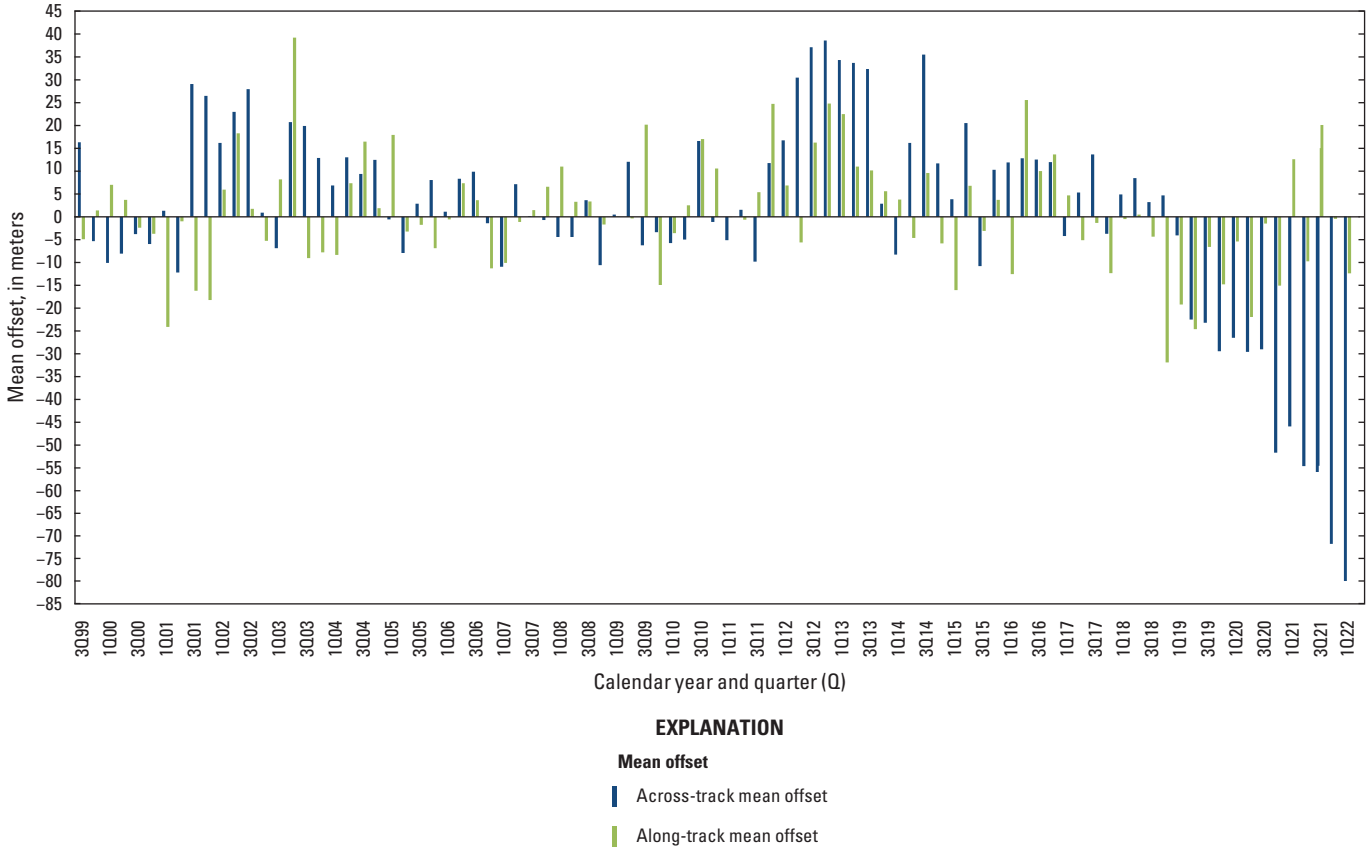

Figure 47. Landsat 7 lifetime mean offsets per quarter.

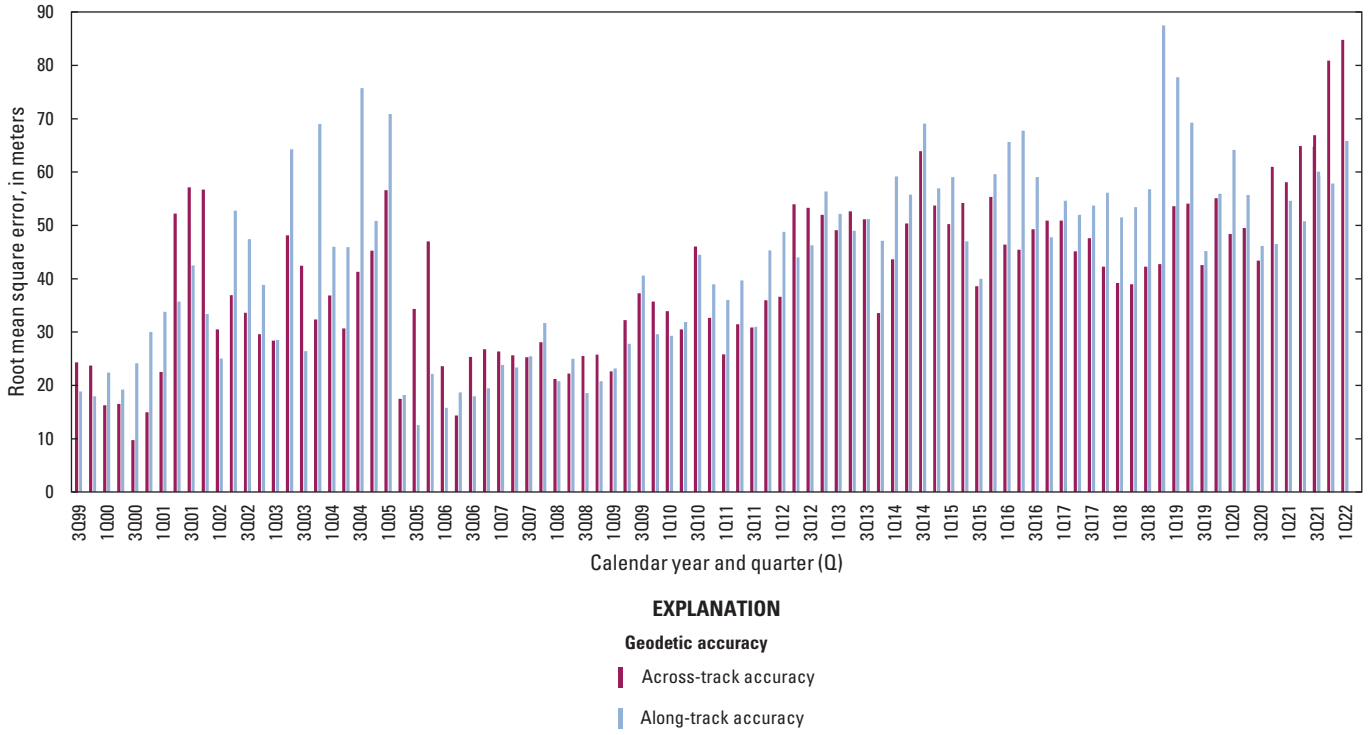

Figure 48. Landsat 7 lifetime geodetic accuracy per quarter.

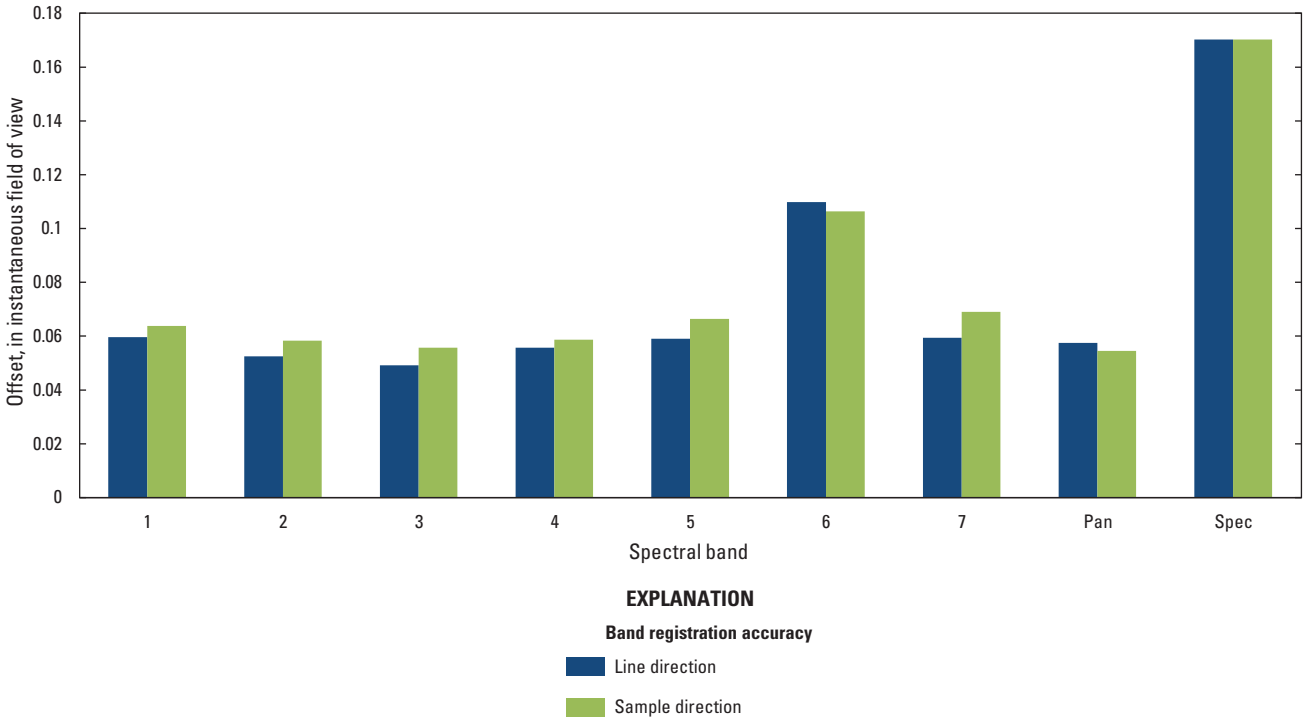

Figure 49. Landsat 7 band average root mean square registration error since launch.

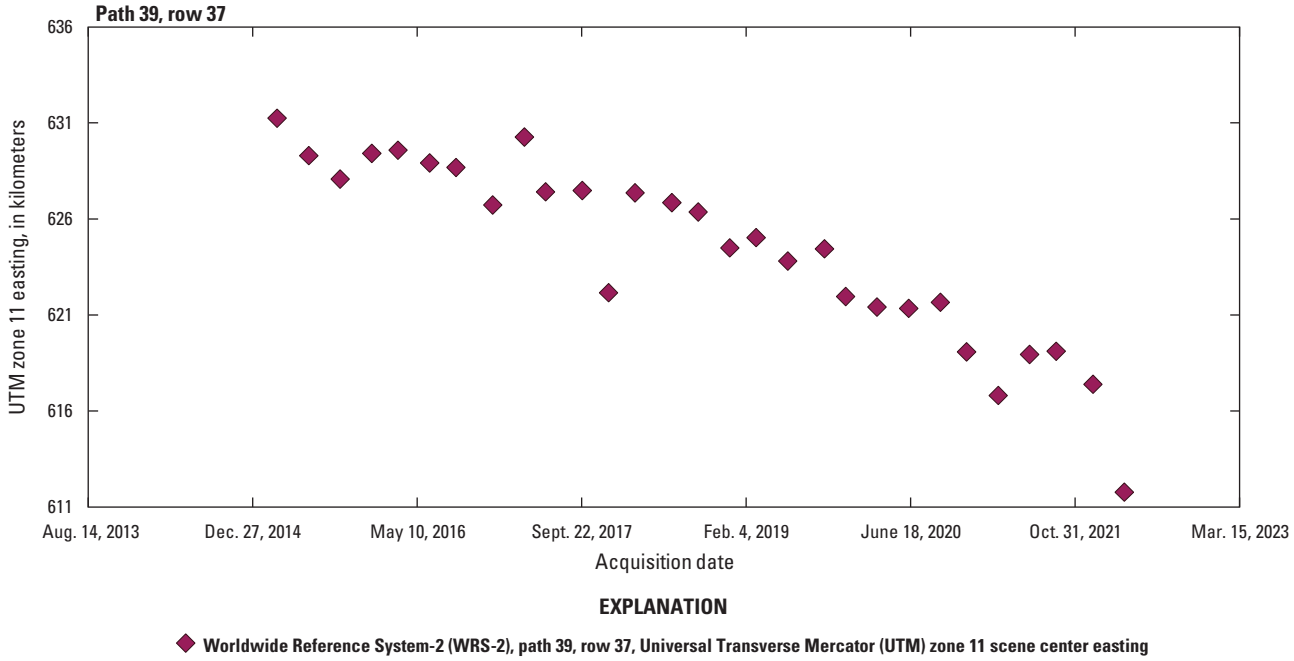

Figure 50. Landsat 7 lifetime orbital drift from World Reference System–2 (path 39, row 37).

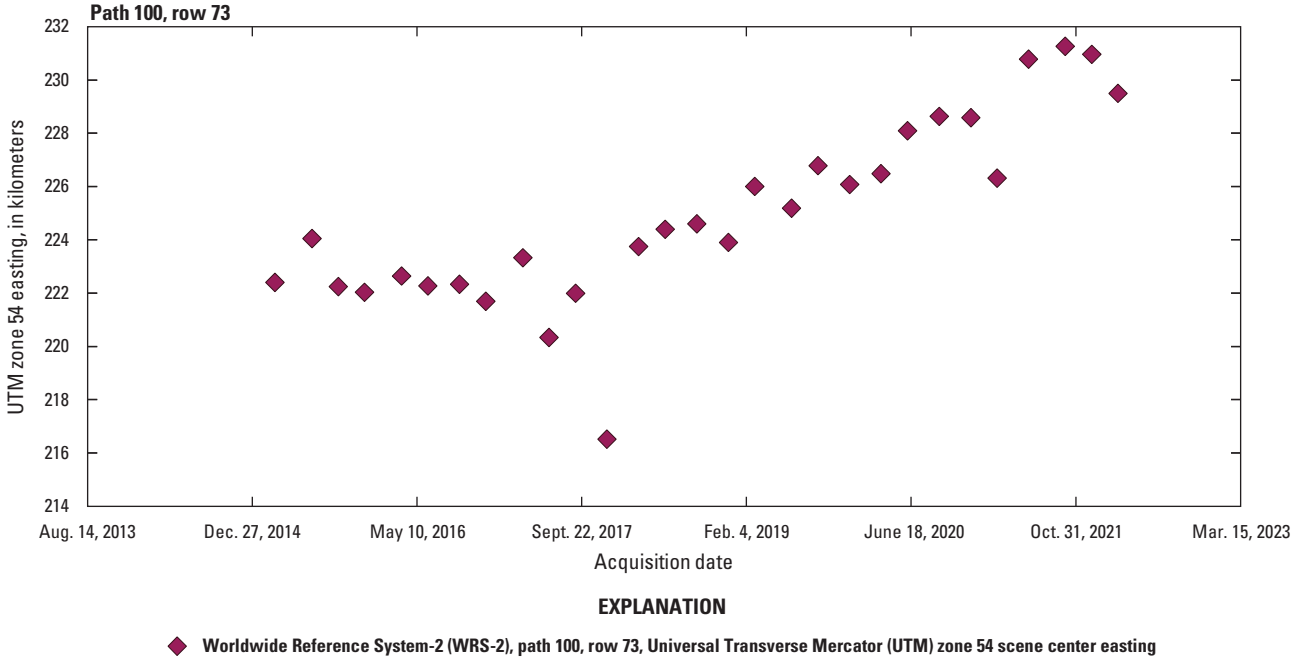

Figure 51. Landsat 7 lifetime orbital drift from World Reference System–2 (path 100, row 73).

Figure 50 shows the observed orbital drift from WRS–2 for path 39, row 37 (33°10′37″ N., 115°38′05″ W.), which is a Northern Hemisphere scene. Magenta diamonds in the figure indicate the scene center location converted to easting and, for historical trending purposes, the measurements begin in 2015. The difference between the first 2015 observation and the most extreme observation from March 2022 is about 19.5 kilometers, at a westward drift.

Figure 51 shows the observed orbital drift from WRS–2 for path 100, row 73 (18°47′14″ S., 138°22′13″ E), which is a Southern Hemisphere scene. Again, magenta diamonds indicate the scene center location converted to easting, and the figure has measurements from 2015 to present. The difference between extreme measurements is about 14.75 kilometers; however, the drift for this Southern Hemisphere scene is to the east.

Quarterly Level 2 Validation Results

Level 2 Surface Reflectance Pseudo-Invariant Calibration Site Trending

In addition to L1 products, Landsat 7 and Landsat 8 surface reflectance PICS trending is performed by the Cal/Val Team. The primary purpose for Level 2 surface reflectance PICS trending is to repeatedly characterize the temporal stability of the ETM+ and OLI sensors. The CNES ROI has been chosen for performing the analysis.

Figure 52 provides the Collection 2, Level 2 lifetime surface reflectance trends for six Landsat 7 spectral bands for the Libya 4 PICS. The x-axis represents time since launch, and the y-axis represents surface reflectance. For this analysis, cloud-free data were used. A strong seasonal effect was noted in the higher wavelength (SWIR) bands (not shown). This seasonal effect has been reduced using appropriate linear

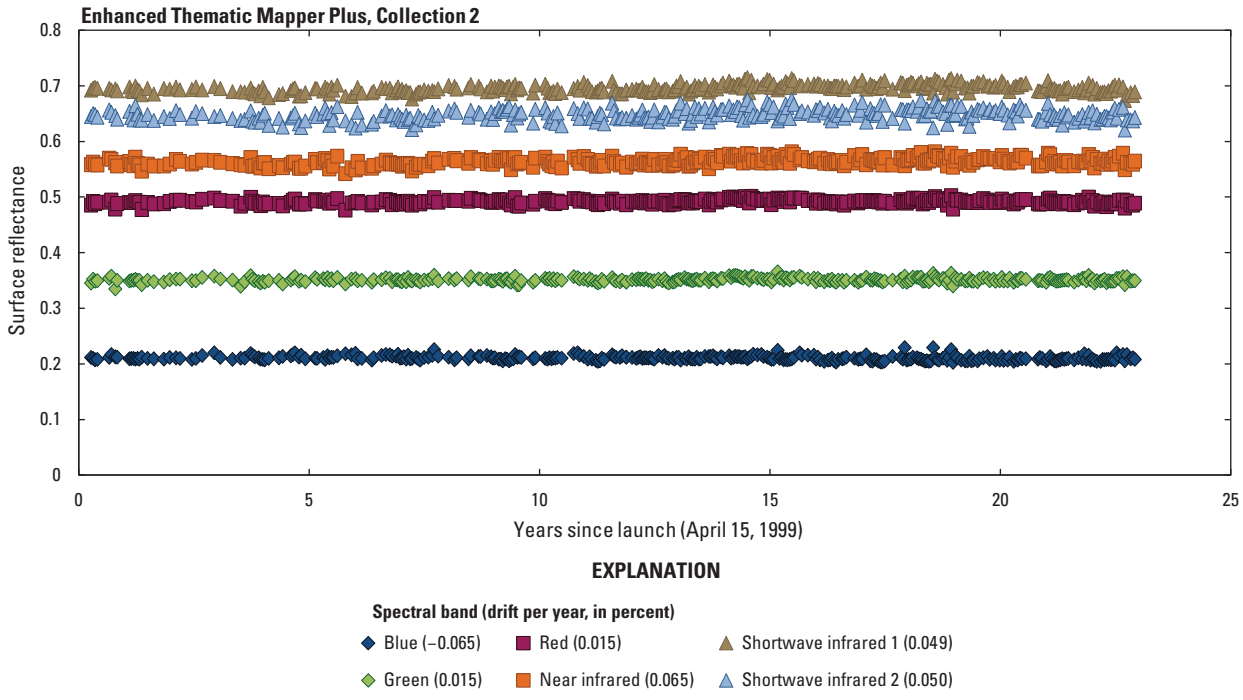

Figure 52. Libya 4 pseudo-invariant calibration site surface reflectance trending, Landsat 7 Enhanced Thematic Mapper Plus, Collection 2.

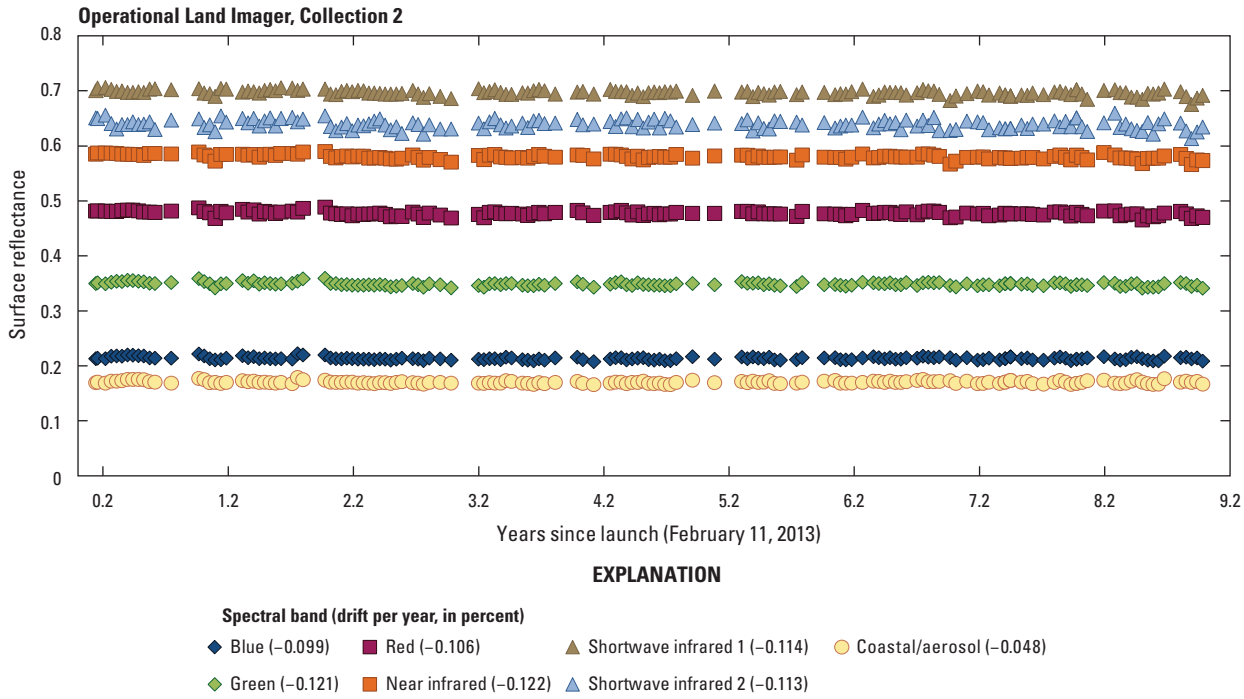

Figure 53. Libya 4 pseudo-invariant calibration site surface reflectance trending, Landsat 8 Operational Land Imager, Collection 2.

models. After reducing seasonality from all bands, drift was estimated for each band from the slope and intercept of line fits. A very small drift was noticeable for each band: a negative drift in the blue band and a positive drift for all other bands. Negative drift solely in the blue band indicates that there may be overcorrection or undercorrection arising from the seasonality removal models.

Figure 53 provides the Collection 2, Level 2 lifetime surface reflectance trends for seven Landsat 8 spectral bands for the Libya 4 PICS. Drift estimate results indicate very small decay in responsivity for all bands. The x-axis represents time since launch, and the y-axis represents surface reflectance. The seasonal effect has been reduced from all bands using appropriate models.

Overall, both OLI and ETM+ showed stability for Level-2 surface reflectance based on the analysis performed. No significant instability was monitored in any band, according to the lifetime drift estimate results.

Summary

The Landsat 8 Operational Land Imager (OLI) and Thermal Infrared Sensor (TIRS) on-orbit radiometric performance for quarter 1 (January–March), 2022, meets all requirements. Geometric performance meets seven requirements and slightly exceeds one requirement. Landsat 7 Enhanced Thematic Mapper Plus (ETM+) on-orbit geometric performance for this reporting quarter meets all requirements. While not measured against specified requirements, Landsat 7 ETM+ on-orbit radiometric performance was fully characterized and summarized in this report. Additionally, quarterly Level 2 validation results for OLI and ETM+ showed stability for Level 2 surface reflectance.

References Cited

Barsi, J.A., Markham, B.L., Czapla-Myers, J.S., Helder, D.L., Hook, S.J., Schott, J.R., and Haque, O., 2016, Landsat-7 ETM+ radiometric calibration status: Proceedings of SPIE Optical Engineering + Applications, San Diego, Calif., 2016, Earth Observing Systems XXI, v. 9972, accessed April 2022 at https://doi.org/10.1117/12.2238625.

Committee on Earth Observation Satellites, 2021, PICS—Pseudo-Invariant Calibration Sites: Committee on Earth Observation Satellites, Cal/Val Portal website, accessed April 2022 at https://calvalportal.ceos.org/pics_sites.

Executive Office of the President of the United States, 2007, A plan for a U.S. National Land Imaging Program—Future of Land Imaging Interagency Working Group: Washington, D.C., Executive Office of the President of the United States, National Science and Technology Council (NSTC) Office of Science and Technology Policy (OSTP) report, 110 p., accessed April 2022 at https://obamawhitehouse.archives.gov/sites/default/files/microsites/ostp/fli_iwg_report_print_ready_low_res.pdf.

Executive Office of the President of the United States, 2014, National plan for Civil Earth Observations: Washington, D.C., Executive Office of the President of the United States, Office of Science and Technology Policy (OSTP) report, 62 p., accessed April 2022 at https://obamawhitehouse.archives.gov/sites/default/files/microsites/ostp/NSTC/2014_national_plan_for_civil_earth_observations.pdf.

Executive Office of the President of the United States, 2016, The second national Civil Earth Observation assessment: Societal benefit areas, subareas, and key objectives: Washington, D.C., Executive Office of the President of the United States, Office of Science and Technology Policy (OSTP) report, 21 p., accessed April 2022 at https://obamawhitehouse.archives.gov/sites/default/files/microsites/ostp/NSTC/the_second_national_civil_earth_observations_assessment.pdf.

Markham, B.L., Ahmad, S.P., Irons, J.R., and Williams, D.L., 1994, Radiometric calibration of the Landsat-7 Enhanced Thematic Mapper Plus: Proceedings of IGARSS '94—1994 IEEE International Geoscience and Remote Sensing Symposium, 1994, v. 4, p. 2004–2006, accessed April 2022 at https://doi.org/10.1109/IGARSS.1994.399636.

Markham, B.L., Haque, M.O., Barsi, J.A., Micijevic, E., Helder, D.L., Thome, K.J., Aaron, D., and Czapla-Myers, J.S., 2012, Landsat-7 ETM+—12 Years on-orbit reflective-band radiometric performance: IEEE Transactions on Geoscience and Remote Sensing, v. 50, no. 5, p. 2056–2062, accessed April 2022 at https://doi.org/10.1109/TGRS.2011.2169803.

Montanaro, M., Barsi, J.A., Lunsford, A., Rohrback, S., and Markham, B.L., 2014, Performance of the Thermal Infrared Sensor on-board Landsat 8 over the first year on-orbit: Proceedings of SPIE Optical Engineering + Applications, San Diego, Calif., 2014, Earth Observing Systems XIX, v. 9218, accessed April 2022 at https://doi.org/10.1117/12.2063457.

National Geospatial Advisory Committee [NGAC], 2020, Landsat data—Community standard for data calibration (October 2020): Landsat Advisory Group, accessed April 2022 at https://www.fgdc.gov/ngac/meetings/october-2020/ngac-paper-landsat-data-community-standard-for.pdf.

Rengarajan, R., Storey, J.C., and Choate, M.J., 2020, Harmonizing the Landsat ground reference with the Sentinel-2 Global Reference Image using space-based bundle adjustment: Remote Sensing, v. 12, no. 19, p. 3132, accessed April 2022 at https://doi.org/10.3390/rs12193132.

U.S. Geological Survey [USGS], 2019a, Landsat 7 (L7) data users handbook (ver. 2.0, November 2019): U.S. Geological Survey, Earth Resources Observation and Science (EROS) Center, LSDS–1927, 139 p., accessed April 2022 at https://www.usgs.gov/landsat-missions/landsat-7-data-users-handbook. [Directly accessible at https://prd-wret.s3.us-west-2.amazonaws.com/assets/palladium/production/atoms/files/LSDS-1927_L7_Data_Users_Handbook-v2.pdf.]

U.S. Geological Survey [USGS], 2019b, Landsat 8 (L8) data users handbook (ver. 5.0, November 2019): U.S. Geological Survey, Earth Resources Observation and Science (EROS) Center, LSDS–1574, 106 p., accessed April 2022 at https://www.usgs.gov/landsat-missions/landsat-8-data-users-handbook. [Directly accessible at https://prd-wret.s3.us-west-2.amazonaws.com/assets/palladium/production/atoms/files/LSDS-1574_L8_Data_Users_Handbook-v5.0.pdf.]

U.S. Geological Survey [USGS], 2020a, Landsat 8-9 Operational Land Imager (OLI)—Thermal Infrared Sensor (TIRS) Collection 2 Level 1 (L1) data format control book (DFCB) (ver. 6.0, September 2020): U.S. Geological Survey, Earth Resources Observation and Science (EROS) Center, LSDS–1822, 58 p., accessed April 2022 at https://www.usgs.gov/landsat-missions/documents. [Directly accessible at https://prd-wret.s3.us-west-2.amazonaws.com/assets/palladium/production/atoms/files/LSDS-1822_Landsat8-9-OLI-TIRS-C2-L1-DFCB-v6.pdf.]

U.S. Geological Survey [USGS], 2020b, Landsat 8-9 Operational Land Imager (OLI)—Thermal Infrared Sensor (TIRS) Collection 2 Level 2 (L2) data format control book (DFCB) (ver. 6.0, September 2020): U.S. Geological Survey, Earth Resources Observation and Science (EROS) Center, LSDS–1328, 72 p., accessed April 2022 at https://www.usgs.gov/landsat-missions/documents. [Directly accessible at https://prd-wret.s3.us-west-2.amazonaws.com/assets/palladium/production/atoms/files/LSDS-1328_Landsat8-9-OLI-TIRS-C2-L2-DFCB-v6.pdf.]

U.S. Geological Survey [USGS], 2021a, EarthExplorer: U.S. Geological Survey database, accessed April 2022 at https://earthexplorer.usgs.gov.

U.S. Geological Survey [USGS], 2021b, EROS Cal/Val Center of Excellence (ECCOE): U.S. Geological Survey website, accessed April 2022 at https://www.usgs.gov/calval.

U.S. Geological Survey [USGS], 2021c, Landsat 7 ETM+ calibration notices: U.S. Geological Survey web page, accessed April 2022 at https://www.usgs.gov/landsat-missions/landsat-7-etm-calibration-notices.

U.S. Geological Survey [USGS], 2021d, Landsat 8-9 Calibration and Validation (Cal/Val) algorithm description document (ADD) (ver. 4.0, January 2021): U.S. Geological Survey, Earth Resources Observation and Science (EROS) Center, LSDS–1747, 807 p., accessed April 2022 at https://www.usgs.gov/landsat-missions/documents. [Directly accessible at https://prd-wret.s3.us-west-2.amazonaws.com/assets/palladium/production/atoms/files/LSDS-1747_Landsat8-9_CalVal_ADD-v4.pdf.]

For more information about this publication, contact:
Director, USGS Earth Resources Observation and Science Center
47914 252nd Street
Sioux Falls, SD 57198
605–594–6151

For additional information, visit: https://www.usgs.gov/centers/eros

Publishing support provided by the
Rolla Publishing Service Center

ISSN 2331-1258 (online)
https://doi.org/10.3133/ofr20221072